**UNIVERSITÀ DEGLI STUDI DI PADOVA**

DIPARTIMENTO DI INGEGNERIA INDUSTRIALE

CORSO DI LAUREA MAGISTRALE IN INGEGNERIA CHIMICA E DEI PROCESSI INDUSTRIALI

**Tesi di Laurea Magistrale in**
**Ingegneria Chimica e dei Processi Industriali**

# HEAT TRANSFER CHARACTERISTICS OF A TWO-PHASE, AIR-WATER DIRECT CONTACT EVAPORATOR

***Relatore: Prof. Alberto Bertucco***
***Correlatore: Prof. Adel O. Sharif , University of Surrey (UK)***

***Laureando: LUCA ZANETTE***

ANNO ACCADEMICO 2012 – 2013

# Riassunto

La mancanza di acqua potabile è uno dei più gravi problemi che l'umanità dovrà affrontare sia a causa del continuo incremento della richiesta sia a causa di un degradamento delle fonti presenti nelle regioni già sottoposte a stress idrico e in quelle in via di sviluppo, come Medio Oriente e Asia.
Innanzitutto, la quantità di acqua disponibile per scopi umani è molto ridotta. Si calcola infatti che il 97.5 percento dell'acqua presente sulla Terra è salata e solo il 2.5 percento è dolce; di questa però meno dell'uno per cento è utilizzabile per scopi umani. In aggiunta, anche i cambiamenti climatici influiscono su questa già precaria situazione, in quanto lo scioglimento dei ghiacciai porta ad una riduzione dei giacimenti di acqua dolce a favore dell'incremento di acqua salata.
L'aumento di popolazione è sicuramente una della principali cause di questa crisi idrica; infatti si stima che la popolazione mondiale raggiungerà gli otto miliardi entro quindici anni, e i nove entro il 2050. Questo aumento di popolazione avverrà oltretutto in regioni con già forti problemi idrici, nelle quali parte della popolazione ha tuttora difficoltà di accesso all'acqua potabile.
Anche le destinazioni d'uso dell'acqua contribuiscono ad aggravare questa situazione, dato che si assiste sempre più ad una competizione tra usi agricoli, industriali e civili che ha effetti devastanti in regioni a scarsa disponibilità d'acqua.
Gli effetti sono riscontrabili in diversi campi, primo tra tutti sulla salute umana; è infatti provato che la maggior parte delle malattie e la loro diffusione sono causate da una insufficiente disponibilità d'acqua: a prova di ciò basta osservare che gli Stati nei quali la situazione sanitaria è peggiore sono anche quelli dove la crisi idrica è molto grave.
La mancanza di una sufficiente disponibilità d'acqua potabile e di servizi ad essa legati può inoltre portare ad una instabilità politica interna e conflitti tra paesi vicini, costretti a dividersi ristrette risorse idriche, come accade tra Israele e Palestina.
Esiste dunque la necessità di affrontare e risolvere, o almeno limitare il diffondersi del problema. Le vie percorribili per questo scopo sono molte, a cominciare da un miglior uso delle risorse disponibili, aumentando quindi l'efficienza degli usi agricoli, industriali e civili, ovvero migliorando infrastrutture e modo di utilizzo.
Una seconda via percorribile è quella dell'aumento della quantità d'acqua dolce disponibile, tramite la desalinizzazione dell'acqua di mare. I processi disponibili per questo scopo sono molti, ma possono essere divisi in due categorie principali: processi a membrana e processi termici. Osmosi inversa (RO), nanofiltrazione (NF) ed elettrodialisi (ED) fanno parte del primo gruppo, il quale sfrutta una forza motrice tra i lati della

membrana (concentrazione o carica elettrica) per produrre acqua dolce. I processi termici invece sfruttano l'energia fornita sotto forma di calore per evaporare l'acqua che viene poi fatta condensare recuperando così anche parte dell'energia. Fanno parte di questo gruppo processi quali *multi-stage flash distillation* (MSF), *multiple effect distillation* (MED) e *vapour compression distillation* (VCD).

I processi appena elencati sono applicati a livello industriale e utilizzati in impianti con capacità produttive elevate, ma esistono altri tipi di processi, che sono in via di sviluppo o applicati in situazioni particolari, nelle quali una produzione di grandi dimensioni non è necessaria né applicabile. Tra queste tecniche si può inserire la desalinizzazione tramite umidificazione-deumidificazione dell'aria (HD). Questa tecnica può essere inserita tra le tecniche termiche, in quanto viene utilizzato del calore, fornito dall'aria o dal liquido, per far evaporare acqua, che viene poi condensata e recuperata assieme ad una parte di calore. Essa presenta diversi vantaggi, primo tra tutti il fatto che l'apparecchiatura necessaria è molto semplice: una colonna per la parte di umidificazione in cui l'aria viene fatta fluire attraverso l'acqua salata in modo da far evaporare acqua desalinizzata, ed una seconda colonna necessaria per la condensazione dell'acqua ed il suo recupero. L'interno della colonna può essere vuoto (colonna a bolle), a riempimento o a piatti; questo permette di ottenere un contatto diretto tra le fasi, aumentando quindi il coefficiente di scambio termico e riducendo allo stesso tempo fenomeni di usura e corrosione dei materiali.

Parte fondamentale del lavoro è rappresentata dallo scambio di energia. I fattori che maggiormente lo influenzano sono le portate di acqua e gas e la temperatura di entrata dell'aria. Le due portate influenzano in maniera rilevante l'idrodinamica della colonna, il *gas holdup* e la dimensione delle bolle, mentre la temperatura di ingresso dell'aria influenza la forza motrice del processo, ossia la differenza di temperatura tra le due fasi a contatto.

Lo scopo di questo lavoro è stato di valutare sperimentalmente come questi fattori incidano sulla quantità di acqua presente nell'aria in uscita, sulle temperature di uscita e sul profilo di temperatura dell'acqua all'interno della colonna. Si è quindi fatta una verifica dei dati sperimentali tramite il bilancio di energia e un successivo calcolo del coefficiente sperimentale di scambio globale di energia. Si è poi confrontato questo valore con delle correlazioni sviluppate da altri autori per valutare se fosse possibile adattare questi modelli al processo preso in esame e si è infine sviluppato un modello per predire il profilo termico dell'aria all'interno della colonna.

La parte sperimentale è stata svolta su una colonna di 7 cm di diametro e un metro di altezza, incamiciata in un cilindro a base quadrata che funge da strato isolante.

Il lavoro è stato effettuato variando i valori di portata d'acqua, portata d'aria e temperatura di ingresso dell'aria. Durante gli esperimenti sono state misurate le temperature in uscita

dell'aria, la temperatura in ingresso e uscita dell'acqua, l'umidità relativa dell'aria in uscita e il profilo assiale della temperatura dell'acqua lungo la colonna.

La successiva parte di modellazione si è svolta prima verificando il bilancio di energia partendo dalla sua formulazione generale e, successivamente, è stato calcolato il coefficiente di scambio di energia utilizzando due diverse formulazioni dell'area specifica, una legata all'area totale e una alle dimensioni della bolla. La seconda parte del lavoro di modellazione è consistito nel calcolare il coefficiente di scambio di energia a partire da due correlazioni disponibili in letteratura, e i risultati ottenuti sono stati confrontati con quelli sperimentali; infine, è stata ipotizzata un'applicazione con una colonna a diametro di un metro, mantenendo le velocità ascensionali uguali ad un caso sperimentale.

I risultati ottenuti sono stati interessanti, in quanto si è riusciti a capire la dipendenza della quantità estratta dalla temperatura di ingresso dell'aria e dalla portata d'aria. Si è visto che, a parità di condizioni, un aumento della temperatura di ingresso dell'aria porta ad un aumento della quantità di acqua estratta. Questo aumento però non è lineare, e dopo un rapido aumento iniziale decresce. Dall'analisi dell'influenza della portata d'aria è emerso che per bassi valori (6 e 8 L/min) si ha un positiva influenza sulla quantità di umidità dell'aria in uscita ma, aumentando la portata, questo effetto scompare tanto che le ultime due portate analizzate (10 e 12 L/min) hanno dato risultati pressoché identici. Si è notata anche un'influenza della portata d'acqua, in particolare un aumento del suo valore porta ad una riduzione della quantità d'acqua estratta.

Non è stato possibile valutare l'influenza di tali parametri sul profilo interno di temperatura dell'acqua in quanto questa temperatura è risultata essere quasi costante.

Questo fatto ha rappresentato un limite per questa analisi che, inoltre è stata effettuata utilizzando acqua di rubinetto come alimentazione invece di acqua salata.

Anche i risultati della parte teorica sono stati interessanti, in quanto si è visto che una delle due correlazioni utilizzate restituiva un errore inferiore al 25 per cento rispetto ai risultati sperimentali, almeno per portate di aria ridotte (6 e 8 L/min). Dall'applicazione del modello si è osservato che la maggior parte dell'altezza della colonna risulta essere superflua, per cui una migliore soluzione è rappresentata dall'utilizzo di grandi vasche con un basso battente d'acqua.

Nel calcolo del coefficiente di scambio termico e nella formulazione del modello sono state fatte alcune semplificazioni, che potrebbero aver inciso sui risultati. Prima di tutto il diametro delle bolle è stato stimato considerando che le bolle fossero sferiche e di dimensioni identiche e che non vi fosse presenza di fenomeni di aggregazione e rottura. Inoltre nella formulazione del modello si è considerata costante la temperatura dell'acqua.

Nel Capitolo 1 è presentata un'introduzione al problema della scarsità d'acqua e successivamente una breve descrizione delle possibili tecniche per la desalinizzazione.

Nel Capitolo 2 è esposta una più accurata descrizione del processo di umidificazione-deumidificazione dell'aria ed, in particolare, della parte di umidificazione. Sono descritti tutti i parametri del processo e la loro influenza sul processo stesso.
Nel Capitolo 3 sono descritte descritta l'apparecchiatura sperimentale e la tecnica utilizzata.
I risultati sperimentali ottenuti sono riportati e discussi nel Capitolo 4.
Il Capitolo 5 espone la parte teorica del lavoro, con l'analisi del bilancio di energia, il calcolo del coefficiente di scambio termico sperimentale e di quello teorico, il confronto tra i due e l'applicazione del modello per la predizione del profilo di temperatura dell'aria.
Dai risultati ottenuti si suggerisce l'utilità della continuazione della ricerca, cercando di ottenere valori più precisi e di valutare temperature più elevate, che possono essere più facilmente ritrovate in situazioni industriali. Un ulteriore miglioramento sarebbe quello di ripetere i test su acqua salata, molto più vicina alle condizioni reali di applicazione.

# Abstract

The purpose of the research was to carry out an experimental and theoretical investigation of the heat transfer on a direct contact column for desalination purposes. The effect of air and water mass flow rates and air inlet temperature on the temperature distribution and moisture content of the air outlet stream was measured. The experimental heat transfer coefficient was estimated and, in order to simulate the experimental results, a comparison with available correlations was performed. The investigated range was from 6 to 12 L/min for air, 2-3 L/min for water and from 30 to 70 °C for the inlet air temperature. Results showed that the amount of extracted water increases with the air inlet temperature. Also the air flow rate influences water extraction, which increases at higher values. The water flow rate affects the residence time, so high water flow reduces the amount of extracted water. Interactions among parameters were observed, and their influence have to be analysed together for a better understanding of the process.

Also the modelling part of the work gave interesting results: it was found that an existing correlation matches very well the experimental value of the coefficient, at least for low gas flow rates. It was also proved that pans with large diameter and small water height would be a better equipment than high columns.

# TABLE OF CONTENT

# Introduction

Water shortage is one of the most important challenges that humanity has to fight because of a continuous increment of water demand, especially in developing countries such as Middle East Asia and Africa, and the deterioration of existing water sources due to intensive usage.

The problem is so relevant also because fresh water availability on Earth is relatively little. In fact, only 2.5% of the total amount is fresh water, but less than 1% is available for human uses, while the largest part (97.5%) is salt water. Moreover, this amount is going to decrease due to climate chances, as glaciers melting will bring to a reduction of the freshwater storage in favour of ocean salted water.

Population growth is one of the main reasons why this crisis is occurring. In fact, it is expected that Earth population will reach 8 billions people in 15 years from now and 9 billions people by 2050, and it will take place in regions where water shortage is already a problem.

Also competition among human, industrial and agricultural usages contributes to emphasize this problem. In fact, both industries and agricultural activities need water, and this water, most of the time, is fresh.

Water shortage badly affects human health; it is proved that most human diseases are caused by insufficient water supply and, in fact, countries where freshwater supply is not enough have the worst health situation.

Additionally, freshwater availability affects also the political stability inside and among countries. The latter can rise when two or more countries have to share a water basin, while fights inside a country occur when water supply is not equally distributed around the population.

The simplest way to overcome this problem is to increase the efficiency of all uses (agricultural, industrial and urban) and, as second option, increase fresh water availability by desalination of the salted water.

The existing processes can be divided into two main groups: thermal and membrane processes. The first one is based on separation of water by distillation: energy is provided to get evaporation. The evaporated water is then condensate and freshwater and heat are recovered. The main processes of this group are multi-stage flash distillation (MSF), multiple effect distillation (MED), and vapour compression distillation (VCD). As about membrane processes, the separation is made by membrane, exploiting their selectivity and permeability. In this group there are three main processes: reverse osmosis (RO),

nanofiltration (NF), and electrodialysis (ED). The last is an electrical potential driven process, while the others are pressure driven.

Beside the main processes, there are some less important ones, which are not widely used. Among them there is the Humidification-Dehumidification process (HD), which is a thermal process that uses direct contact heat exchangers in order to evaporate and condensate water. The advantage of this technique is that the heat duty could be provided by some waste energy sources, such as waste combustion gases or exit coolant fluids. Moreover, the equipment needed is simple and also the maintenance and operative costs are low. So the application of this process is interesting and could provide a very cheap way to obtain freshwater.

Water extraction occurs in the humidification step, where water is evaporated thanks to an air flow rate that provides the heat needed. For evaporation to take place the heat transfer plays an important role and understanding its behaviour is very important.

The aim of this work is to measure the heat transfer rate and the influence that main process parameters have on the exit temperatures, the total amount of extracted water and the temperature profile inside the column. A mathematical model able to predict the air temperature profile knowing the initial condition is also developed.

In the first chapter of the thesis work a general overview of the water shortage and its consequences are shown. Moreover, a general introduction to desalination is presented and descriptions of the main processes are proposed. In the second chapter a general description of the HD process is presented, then a deeper analysis of the influence of the process parameters on water extraction and heat transfer is carried out. Chapter Three describes the used equipment and the experimental procedure. Obtained data are presented and discussed in Chapter four. In Chapter five a calculation of the experimental heat transfer coefficient is carried out, then a modelling of the process is proposed comparing different heat transfer coefficients.

I would like to thank the University of Surrey for giving me the opportunity to do my dissertation there; Prof. Adel Sharif, Dr. Sami Mohammed and Hameed Mahood for the support they gave me during all my period in their department.

# Chapter 1

# Desalination

In this chapter a review of water shortage problem is presented. Then it is also shown all the main techniques available for overcoming this problem. The first solution presented is the thermal desalination, and then the membrane one.

## 1.1 Water shortage

Water shortage is one of the greatest challenge that human beings has to fight in order to maintain and increase quality of life. In fact, even though more than 70% of the Earth surface is covered by water, only 2.5% of this water is fresh water and the remaining 97.5% is stored inside oceans, as shown in Figure 1.1a. Moreover, more than two third of the total fresh water is stocked in ice packs and glaciers, the 30% in the underground and 1% in the high latitude permafrost. The remaining 0.4% of the total fresh water is distributed among lakes (about 66%), moisture (12%), atmosphere (9.5%), wetlands (8.5%), rivers (1.5%) and vegetation (1%), as Figure 1.1b shows.


*Figure 1.1a: water percentage distribution in the world*

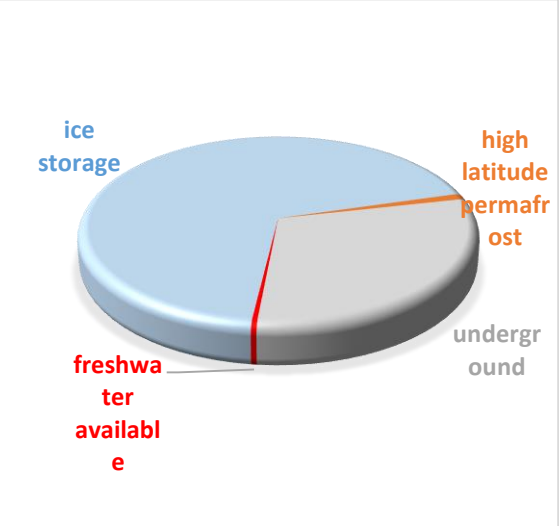


*Figure 1.1b: freshwater percentage distribution in the world*

In addition, available freshwater is not equally spread around the world and some areas, such as sub-Saharan Africa, West Asia and North Africa, have been already suffering water shortage for a long time.

Beside this there are also environmental changes that will affect water availability in the next years. It is very well known that world's mean temperature is increasing very fast and it is estimated to increase more in the future years. This will cause a progressive retreat of the glaciers, and a consequent decrease of freshwater amount in favour of seawater. This phenomenon will be dramatic for those countries where melted ice is one of most important freshwater sources, such as Andes and Himalayans areas.

World's population increase (8 billion by 2025 and 9 billion by 2050) is one of the greatest factors affecting this problem. This very quick growth will take place in the developing countries, such as China and India, where water demand will exceed supplies in less than 20 years.

Another important aspect is water consumption due to urban activities, industry and agriculture. Agricultural activities have a great impact on water consumption due to the large amount necessary for irrigation purposes. Moreover, with the change of dietary preferences, this amount of water is estimated to reach 1000 $Km^3$ per year by 2025, which is 20 times the current flows on Nile.

Human daily activities waste a large amount of water due to lacks in the distribution systems, which cause a loss of about a third of the circulating water. Another source of waste is the excessive water usage in the most developed countries.

Water shortage has also effects on political stability among countries, and an example of that is the fight between Israelis and Palestinians. This and other fights rise also from the fact that they have to share freshwater basins, which often are the only available source of water.

Beside conflicts among countries, a water scarcity could lead to instability also inside countries, as civil wars in African states proved. In those countries water prices are very high, and only the upper class can afford them, causing the rising of tensions with the other classes.

Water scarcity also influences quality of life, especially food availability and health. In fact, famines are caused by a water absence and it is proved that around 80% of the world's diseases are caused by inadequate water supply. In addition, energy is strongly dependent on water availability because a lot of countries use it to generate electricity.

It is clear that some reliefs have to be taken. One important thing that could help is setting up precise rules, in order to decrease conflicts risk.

In addition, a better management of the available water can improve the situation too. For example, an efficient irrigation can reduce the wastefulness; the improvement of the structures can decrease the loss of water during the pumping and the concept of water

reuse must be introduced, even though the latter has some psychological constrains, especially in the developed countries. Next to this, a better "water usage education" must be developed, in order to avoid water waste for domestic and industrial purposes.
After these simple but important solutions, some alternatives aiming to increase the amount of water could be taken into account. One of these techniques is the desalination. It can be applied in seawater, brackish water, and geothermal water and consists on extracting the dissolved salt in order to make water useful for human purposes.

## 1.2 Water Desalination

Desalination is the widest used technique for freshwater production because its basics are very simple: purify water extracting salts and other suspended and dissolved solids to obtain a water suitable for human and agricultural purposes.
Available techniques for freshwater production are divided in two main categories: membrane and thermal processes. The formers are based on separation through membranes exploiting their permeability and selectivity. Main processes of this group are reverse osmosis (RO), electrodialysis (ED) and nanofiltration (NF). Thermal processes instead are based on providing energy to get water evaporation and then recover it by condensation; multi-stage flash (MSF) and multiple effect distillation (MED) are part of this group. A deeper analysis of all these processes is proposed in Paragraph §1.3.

Feed water salinity has a very wide range, but it can be divided into two main categories: seawater and brackish water. The latter is characterized by a salt concentration of 1000-10000 mg/L and can be found in the estuaries and on groundwater in salty aquifers, while for seawater the typical salt concentration is 10000-60000 mg/L (Greenlee, et al., 2009). If the concentration is lower than 1000 mg/L the water is considered freshwater, but it does not mean that this water is drinkable, because drinkability depends on the single state rules. This is a very important factor in the choice of a plant, because not all the techniques are suitable for all the salinity range.
Beside this, there are other factors that have to be taken into account in the design of new plant, such as required product quality and site characteristics, which include energy and labour cost, available area and local demand for electricity.
Thermal driven processes are suitable for high feed salt concentration, while membrane processes have some limitations due to rising problems regarding both membranes and operating conditions. In fact, the higher salt concentration is, the higher pressure has to be given to the system and consequently the higher is energy demand and membrane degradation.

As about water quality, thermal processes can gain better results because salt cannot come out with vapour and so the product is almost pure water. In membrane processes, product quality is greatly affected by the membrane performances because salt can flow through the layer and come out with the product. Moreover, these performances are not constant during plant life due to a decay of the material. It means that continuous controls have to be made and membranes have to be changed periodically.
Thermal processes maintenance is simpler than membrane ones, because the main problem is the fouling, that can be easily fixed with periodical cleaning.
Life of plants is another point in favour of thermal processes. Currently, a thermal plant life is expected to be around 20-30 years, and after that period, it can be easily upgraded only replacing the damaged pieces, maintaining the main structure. For membrane processes, this is not so easy, because of the fast developing of this technology could bring to a fast change of the process layout.

Another term of comparison is the final water price. In fact it is estimated that it is around 0.5 US$/m$^3$ for biggest plants (Fritzmann, et al., 2007) (Al-Sahali, et al., 2007) for both kind of processes. In any case, the lower the size of plants is, the higher the total cost of the water. The increase is smaller for thermal processes, which can be considered almost independent from the quantity. This is one of the reason why thermal processes are preferred to membrane ones when the water demand is low.
The main point in favour of membrane process is the amount of operative costs, which are much lower than thermal processes one. This is the main reason why membrane have been widely used is areas in which energy costs is high while thermal ones are the main choice where energy has a low price.

As it can be seen in Figure 1.2, desalination plants are spread all over the world, in particular in those regions in which water scarcity is a problem all year long or only for limited periods. Trend during the last years has been to prefer membrane technologies because of their lower operating costs and energy requirement. In fact the 80 % of the installed plants are based on membrane processes and only 20 % on thermal ones. Despite this data, thermal processes count for 50 % in the total water production. This is due to higher efficiency of these processes and to the size of the installed plants.
In Europe most of the plants (about 75 %) work with a membrane technology and they are mainly located in Mediterranean coast countries, such as Italy and Spain, which together have the 2.6 % of the world freshwater production. Desalination plants can be found also in Countries were sunshine is lower, such as France and United Kingdom.

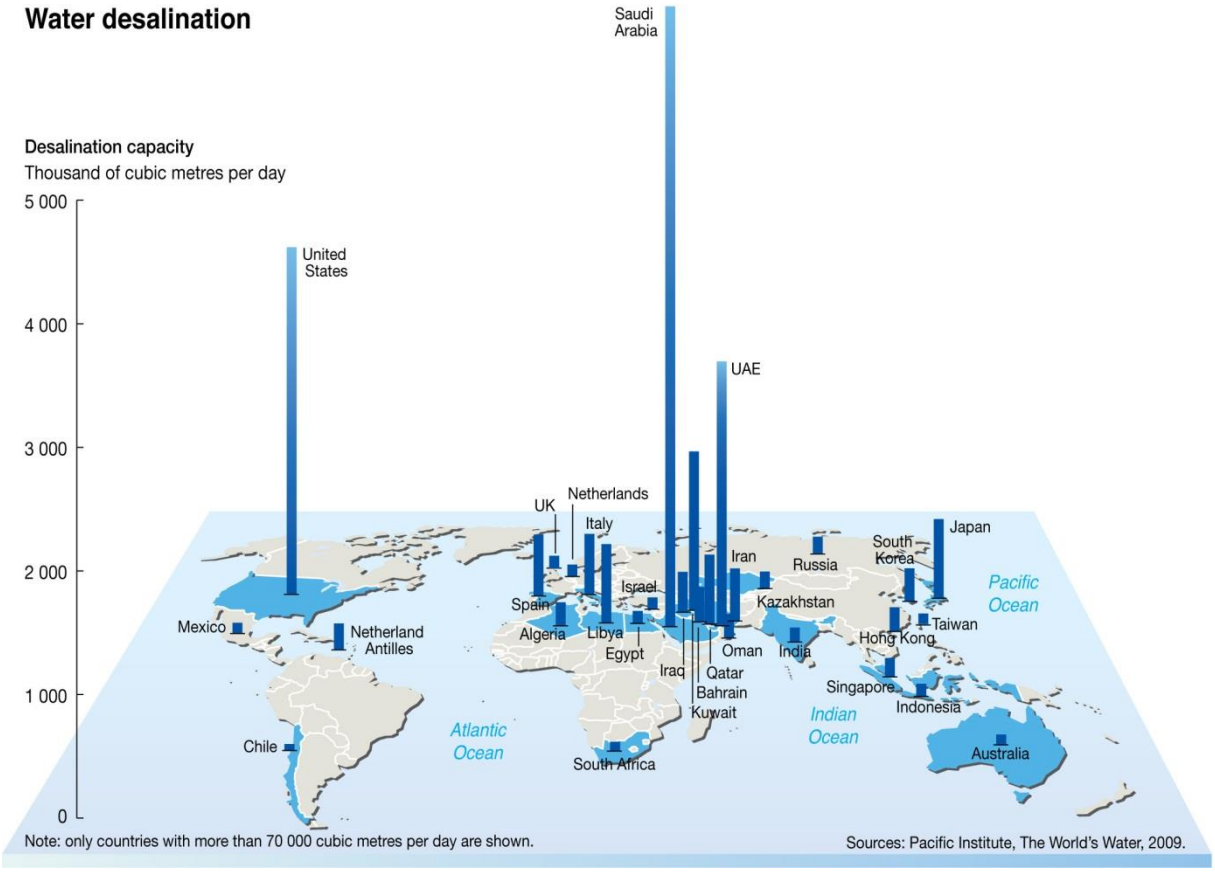


*Figure 1.2: freshwater production around the world*

Eastern Asia desalination leader is Japan, with 3.7 % of the global freshwater production. This data is going to change due to the great population and industrial growth occurring in this part of the continent. This change will regard mostly China, in which water demand is expected to exceed the current supply and so desalination will be one of the most important solutions.

As about America, US are the second world freshwater producer, in fact they count for the 17 % of the total, and two thirds of these are reverse osmosis plants.

The area where desalination is most widely applied is the Middle East, particularly in the Gulf States. The 50 % of the world desalination capacity (2000) is stored in this region. In particular, Saudi Arabia is the greatest producer in the world, it counts for 26 % of the total amount of water even though its population counts only for the 0.4 % of the total. Desalination is widely used also in the United Arab Emirates, which are the third world freshwater producers.

Despite the world's trend, in this region thermal processes are the mostly used and the main reasons are the low cost of fossil fuel and the poor feed water quality, which has very high salt concentration and a high fouling potential. In the Gulf States, water

desalination is often coupled with electric power generation, in order to increase the energy efficiency of processes.

## 1.3 Thermal Processes

These processes have been the first to be developed and they have been applied since 1881, when the first inshore plant was established in Tigre (Malta, Figure 1.3). Moreover, this kind of processes have been the only desalination process installed until around the middle of 1980 (Greenlee, et al., 2009) (Fritzmann, et al., 2007).
Later, the incoming of the new membrane technology caused a reduction of number of installations, even though the efficiency of thermal processes is higher than membrane ones.
One of the reasons that allowed distillation processes to have a great diffusion is the very well-known basics behind them: the principles of distillation. The main idea of this kind of processes is to provide energy to the feed water to get evaporation and then condensate this steam to both obtain freshwater and energy recovery.
The main problem of this kind of processes is the greater amount of energy necessary for the separation, as the amount of energy required is equivalent to the latent heat of vaporization of water. However, because of the great results that this kind of processes can achieve, researches are carried out to improve energy saving and find new energy sources for the necessary energy.

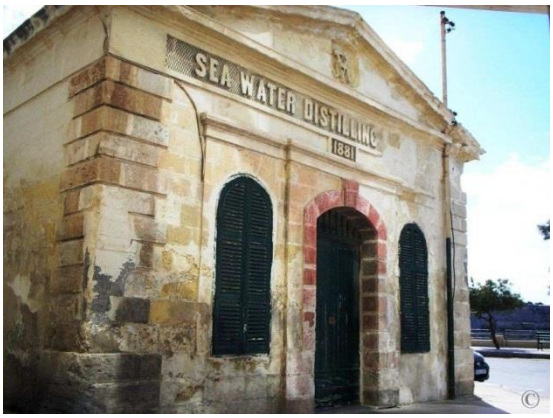


*Figure 1.3: remains of the first desalination plant in Tigre (Malta)*

### *1.3.1 Multiple-effect distillation (MED)*

Multiple effect distillation (MED) is the first developed thermal process and it has been used, in small application, since the XIX century. This process is an evolution of the simple distillation process, and it was developed to increase the amount of produced water decreasing the running costs.

It consists of a succession of chambers (called effect) in which seawater evaporates. As it can be seen in Figure 1.4, energy required for the evaporation is given by the steam formed in the previous effect or, as far as the first chamber, by a boiler.

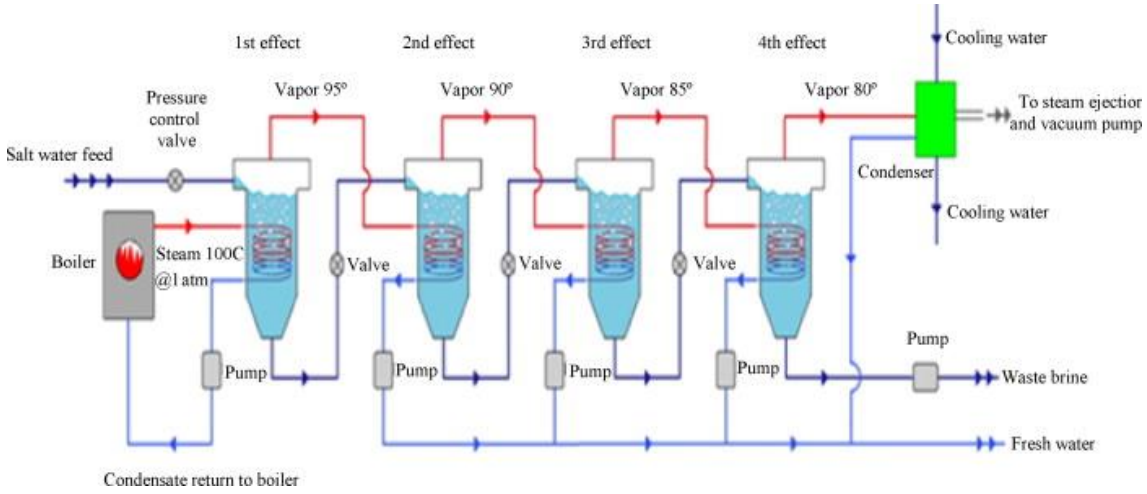


*Figure 1.4: layout of a simple MED process*

In order for evaporation to take place in each effect without providing heat, it is necessary to have a decreasing vapour pressure during the process. This is made by decreasing pressure in the feed side with valves, placed before the feed inlet. After the last effect, lasting steam is condensed with cooling water and vacuum pump and ejectors are put to maintain the necessary pressure and the steam circulation. Presence of incondensable, such as dissolved gas, is dangerous for the process because it decreases heat transfer coefficient and modifies the pressure inside the effects. To avoid all problems, a vent system is necessary too (Saidur, et al., 2011).

### *1.3.2 Multi-stage flash distillation (MSF)*

Multi-stage flash desalination is the most widely used thermal desalination technique thanks to the simplicity of the process and its management. It is very similar to the MED, because it uses the generated steam as an energy source, but MED uses this heat directly for water evaporation, while MSF uses this heat for preheating purposes. In MSF evaporation is obtained with a liquid lamination. Heat provided by the steam is not enough to reach boiling temperature, so a boiler is necessary too.

Boiler is the first step after the pre-heating, and then feed seawater is laminated many times as the number of stages. At any lamination corresponds a water pressure decrease and so a water partial flash.

At the end the total amount of freshwater is collected and sent to the post-treatments, while the brine is sent to the brine disposal (El-Ghonemy, 2012) and the remaining vapour is condensed to increase the energy recovery. In Figure 1.5 is shown a layout of a MSF process.

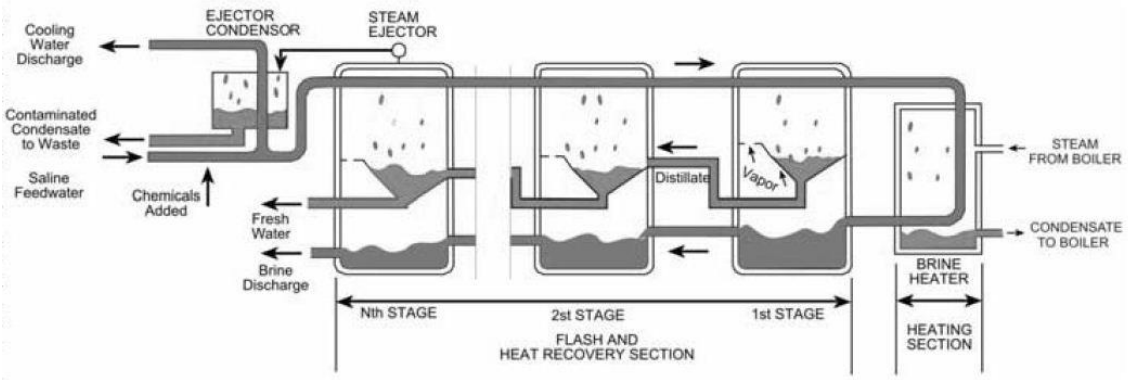


*Figure 1.5: layout of a MSF process*

The greatest advantage of this technique is that the process is very simple and it is possible to obtain a great amount of freshwater with a single boiler.

Potentially this process has no limits, in fact increasing the feed temperature increases the amount of freshwater production but there is a limit due to scale formation. For that reason, this kind of plants usually works between 90-120 °C to avoid the formation of precipitates (El-Ghonemy, 2012).

### *1.3.3 Vapour compression distillation (VCD)*

This technique is very similar to the other previously mentioned. The greatest difference among them is that in VCD the initial heat is not given by a thermal source, but it is given by a compression of the steam leaving the last effect. This compression increases the steam temperature but it is also the most expensive part of the process. The schematic process diagram of the process is shown in Figure 1.6 (Al-Sahali, et al., 2007).

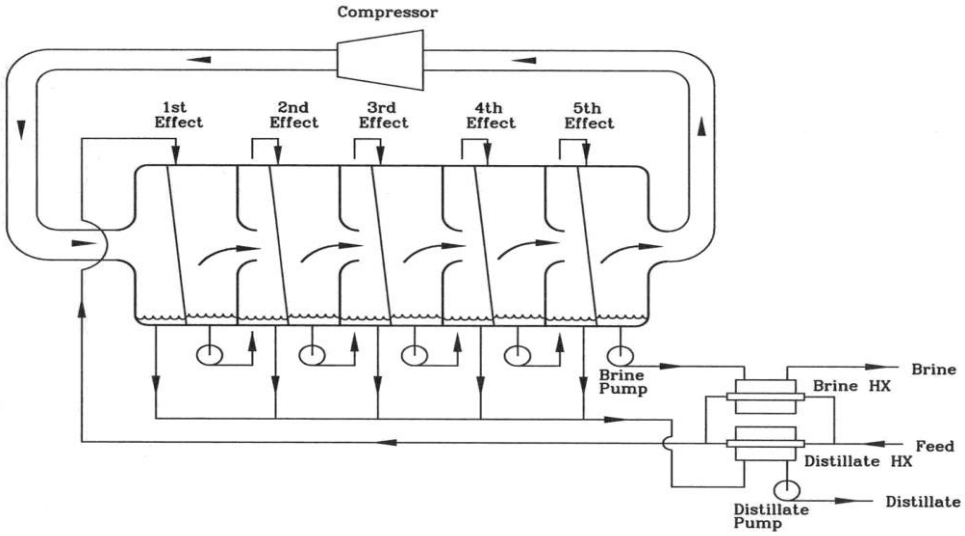


*Figure 1.6: simplified process diagram of a VCD process*

## 1.4 Membrane processes

The first membrane applications have been developed since the ‘60s, but they started to have great importance from the middle of the ‘80s and now they are the widest used techniques around the world. What allowed membrane processes to become the main installed process was the great efficiency improvement obtained thanks to technology development. This gave the possibility to obtain good products with low energy consumption, which is the main disadvantage of their counterpart.

As mentioned, those processes are based on extracting salts and other impurities applying a driving force, which is pressure for RO and NF, while ED is driven by an applied electric field that causes ion movements. After the separation, permeate (freshwater) is extracted and retentate (brine) is send to specific treatments, due to specific disposal rules.

The flow-sheet of membrane processes is almost the same, and it is shown in Figure 1.7. It consists of:

- Water abstraction from the sea. There are two available ways: coast and beach wells or open seawater intake systems. The former provides a better water quality (less turbidity) but requires more space, (1);
- Pre-treatments. They are necessary to adjust the intake water in constitution and pH value, (2);
- Membrane unit. This is the part of the plant that diversifies each kind of process mainly, (3);
- Post-treatments. In this section freshwater is re-mineralized, re-hardened and adjusted to drinking water standards, (4);

- Control system. This is necessary to guarantee that the standards are always respected, (5);
- Brine treatments and disposal. The concentrate cannot be re-intaken inside the sea directly, (6).

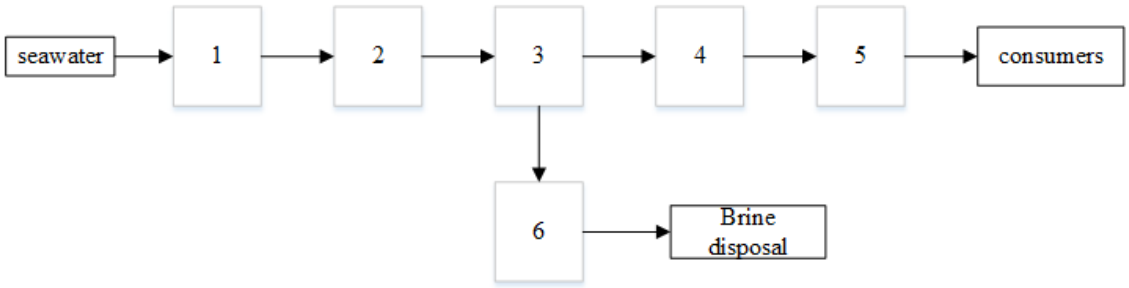


*Figure 1.7: typical layout of a membrane process*

In many plants, due to energy costs, it is found an energy recovery system too. This is not necessary for the process, but it is very useful to save energy costs.

### *1.4.1 Pressure driven processes*

Both RO and NF are pressure driven processes, what diversify the two processes is the range of rejected salt molecular weight and the characteristics of the membranes.
The applied pressure pushes the water through the membrane and this allows separation to take place.
This applied pressure must be higher than the osmotic one, which is one of the most important parameters in the pressure driven processes. It is defined as the hydrostatic pressure generated by the difference of liquid height that is reached at the equilibrium between the two sides of an osmosis process.
This property depends on the fluid and the dissolved concentration of solids inside of it. For a thermodynamically ideal solution, the expression of this property is:

$$\Pi = CRT; \tag{1.1}$$

where C is the molar concentration (kmol/m$^3$), R the ideal gas constant (J/kmol K) and T the operating temperature (K).
As it can be seen in Equation 1.1, osmotic pressure is deeply linked with temperature and concentration of the solution. Both a temperature and concentration growth increases the osmotic pressure, and consequently the operating pressure. Typical values of osmotic pressure are 2300-2500 kPa for seawater (but can be up to 3500 kPa), and 100-300 kPa (2000-5000 mg/L) for brackish water.

During a desalination process, when a pressure higher than osmotic pressure is applied, the reverse osmosis process takes place and water goes from the concentrate side to the diluted one instead of vice-versa. In figure 1.8 it is shown the reverse and the forward osmosis principle; it is also shown how a graphical interpretation of the osmotic pressure.

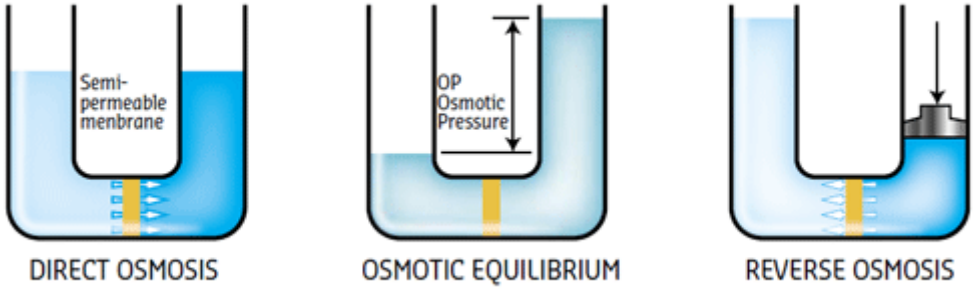


*Figure 1.8: basics of the direct and reverse osmosis*

The amount of freshwater recovery is an indicator of process performance and it is expressed as:

$$R_W = \frac{Q_P}{Q_F}; \tag{1.2}$$

Where $Q_P$ ($m^3/h$) is permeate volumetric flowrate and $Q_F$ ($m^3/h$) is the feed volumetric flowrate.

The amount of freshwater achievable depends on both operating pressure and membrane properties. The most important are the permeability (expressed in terms of permeability coefficient) and selectivity, which can be expressed as shown in Equation 1.3 (Wijimans, et al., 2005) and 1.4 respectively:

$$L = \frac{D_a SV}{RTl}; \tag{1.3}$$

where $D_{ab}$ is the water diffusivity ($m^2/s$), S is the water solubility (kmol/ kmol sol), V is the water partial molar volume ($kmol/m^3$) and *l* the membrane thickness (m). As it can be seen in Equation 1.3, temperature plays an important role on the permeability of membranes, in particular an increase of 1°C causes an increase of 3 % of the flux. This is due to an increase in the diffusivity, which is dependent on temperature with a coefficient greater than one.

$$Sel = \frac{moles\ of\ desired\ product}{total\ mole} \tag{1.4}$$

Amount and quality of permeate are linked with these two membrane properties. In particular high flux means low selectivity while low flux means high selectivity and during operations it is necessary to find a compromise between them. The amount of water flowing through the membrane ($N_A$, kmol/hm$^2$) can be expressed as:

$$N_A = L(\Delta P - \Delta\pi) \tag{1.5}$$

Where L is the previously mentioned permeability coefficient, ΔP is the transmembrane pressure difference (Pa), Δπ is the osmotic pressure difference between the influent and the permeate.

Water can flow through membrane with two different mechanisms: convection and diffusion.

Convective transport is the main mechanism of the porous membrane, in which water can flow inside the canals, while diffusive transport is the typical transport of the nonporous membranes, in which the absence of canals allows only this mechanism.

Description and prediction of these mechanisms are important, especially for the design of the process. As about the convective transport, there are many models available, while the diffusion mechanism is described with the so called solution-diffusion model. This transport model divides the process in three main steps: absorption onto the membrane surface, diffusion through the thickness of the membrane, and desorption from the permeate surface of the membrane ( Paul, 2004).

Beside the main water flux, there is always a salt flux too, due to the imperfect rejection of membranes. This flux of salt can be predicted knowing the bulk concentration of salt. However, there is an important effect that must be taken into account during the design of this kind of processes: the concentration polarization. It rises during the operation, when the concentration of the feed solution increases, and it causes an increase of salt concentration near the membrane surface. This is due to two main reasons, one is the chemical nature of the membrane and the other is the salt slow counter flux to the bulk after the rejection. This high salt concentration increases the real driven force between the two membrane sides, increasing consequently the real flux of salt.

A problem linked with this kind of process is the membrane decline. It is reported that membranes lose 10 % of their salt rejection every year and so it becomes necessary to replace them about every 7 years.

Performance decay is also linked to the salinity of the feed water. In fact, the higher the feed salinity, the higher stresses that membranes have to sustain. Stresses are linked to both applied pressure and necessary work for the rejection.

### 1.4.1.1 Reverse Osmosis

Reverse osmosis is the most widely used membrane technique, but it can be also applied for other purification purposes, such as for treatment of effluent water and separation of organic compound.

As mentioned, the applied pressure must be higher than the osmotic pressure; typical value of applied pressure is 6000 – 8000 kPa for seawater RO (SWRO) and 600 – 3000 kPa for brackish water RO (BWRO) (Greenlee, et al., 2009).

The reason why this technique is so widely used for desalination is that it can reject also compounds with lower molecular weight, including monovalent ions. This separation is possible thanks to membranes action, which are the most important part of the plant. In order to obtain industrial scale production, membranes are required to have high fluxes and high rejection. The best available membranes to achieve this goal are the thin ones. These membranes are assembled of two different parts: a nonporous active part and a porous one, which has the function of protecting and giving physical support to the nonporous part, which is the real important part for the salt rejection.

This active layer is usually made of polyamide, produced by interfacial polarization. As about the structure, there are tortuous canals in which water has to diffuse in order to pass the membrane. In these thin and tortuous canals, salt or ions cannot flow and only water is able to diffuse and overcome it.

The porous layer is made of micro or ultra-filtration membranes.

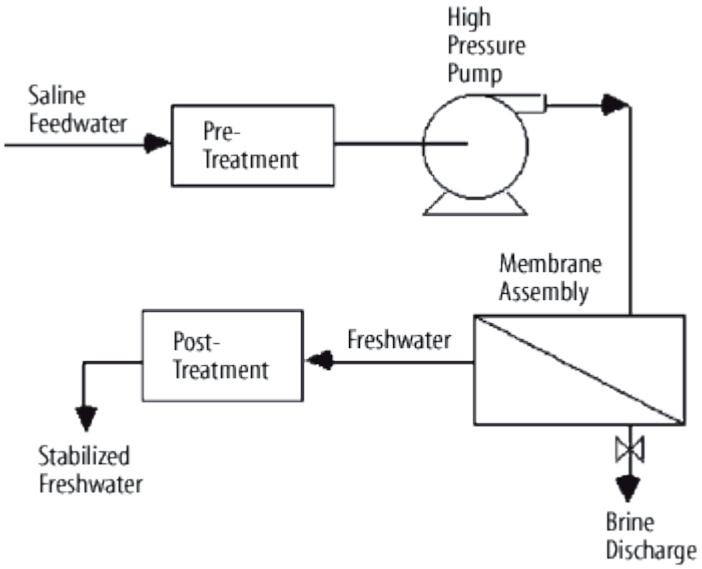


*Figure 1.9: layout of a RO desalination plant*

The introduction of composite membrane led to an increase of desalination performances and physical stability, a stronger resistance to bacteria degradation and a higher stability in a wide range of feed salinity and flow-rate. In addition, water recovery increased

greatly during the years insomuch as today it is possible to achieve a percentage greater than 99.6% (Fritzmann, et al., 2007).
In Figure 1.9, it is shown a typical layout of a RO process while in Figure 1.10 a detail of a membrane.

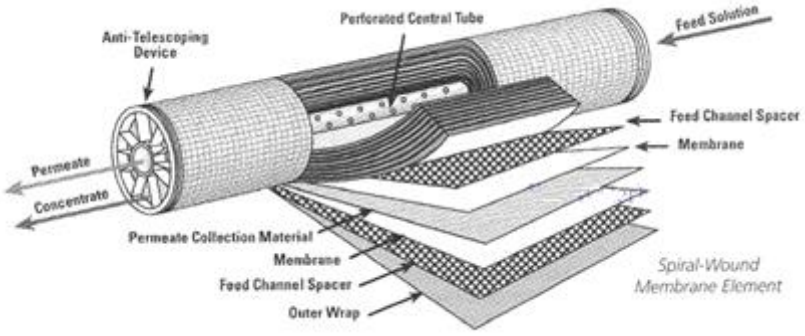


*Figure1.10: detail of a spiral wound element*

The usually installed membranes are spiral wound elements (Figure 1.10) because they offer a great surface to volume ratio and more mechanical resistance than other layouts.
These kinds of membranes are able to reject particles with a molecular weight much smaller than 200 g $mol^{-1}$, including the monovalent ions, such as $Na^{+}$.

### 1.4.1.2 Nanofiltration

Nanofiltration (NF) is an alternative to the RO processes and it can be used with both seawater and brackish one, but as far as the former, it is not enough to achieve the standards required by drinkable water. A new and powerful use of this technique is as pre-treatments for a RO process. This use brings to a chemicals and energy reduction and to an increase of water recovery. A pre-treatment made with NF could remove more than 57 % of the total TDS (total dissolved solids) (Bird, et al., 2007). This allows a cost reduction for the RO unit in both capital and operating costs and a general reduction of production costs due to the lower price linked to the NF process.
Lower costs are one of the advantages linked to NF and it is why this technique could be preferred to RO, especially for BWRO. In fact, for this kind of feed water, NF it is proved to be able to achieve drinkable standards. Other advantages are that operating pressure is lower compared to RO process and the flux through membrane is higher.
Membranes used for NF are porous ones, with pores of nanometers size. They are able to reject dissolved solids with molecular weight higher than 200 g $mol^{-1}$, including

multivalent ions, such as $Ca^{++}$ and $Mg^{++}$, responsible for water harnesses. This technique is able to remove sulfites, nitrites, and metal ions. It is also widely used to remove both turbidity and microorganisms placed inside water.

NF can be also coupled with thermal processes. In fact, it can be used before the evaporative units as pre-treatment. In this way, it is possible to remove great part of the suspended solid and salt concentration, and thermal process is used only to remove the remaining part. This brings to a reduction of the total amount of required energy and a reduction of the risk of scale formation, and process temperature can be kept higher, removing the limit showed in the previous Paragraph §1.3.2

## *1.4.2 Electrodialysis process*

Elctrodialysis is the third main membrane process and, differently from the others, the driving force is an electrical potential difference. This technique has been used since the '60s and sometimes it is preferred to RO process, especially in those regions in which water source is deep located or hardly supplied with chemicals.

This technique is preferably used for brackish water because salt concentration is lower and consequently a lower applied potential is required. There are many advantages linked to this technique; one is that the water recovery is very high because it is possible to work beyond the saturation point. Other advantages are that it is possible to vary the product water quality simply changing the applied potential difference. Moreover, this kind of process is less affected by feed water constituent and contaminant.

In Figure 1.11 it is shown how the ED unit is made and how it works. The desalination unit is made of a series of alternate anion and cation exchange membranes. At the end of the membrane series there are two electrodes, necessary to create and maintain the necessary driving force ( Sadrzadeh, et al., 2008).

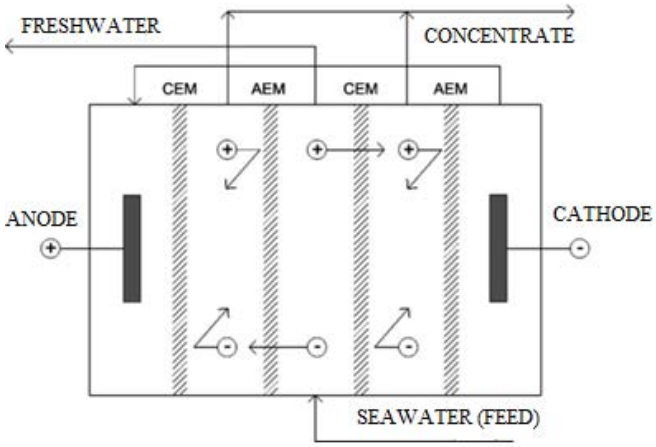


*Figure 1.11: electrodialysis scheme*

Water is fed in all of the compartments and an electric potential is applied between anode and cathode. This causes ions movement, in particular cations move to the anode while anions move to the cathode. This movement is allowed by membranes; in particular cation exchange membrane (CEM in the figure) allows cations movement while AEM (anion exchange membrane) allows anions passage. This ions movement at the end of the process causes a succession of concentrate water and freshwater. The concentrate one is taken and sent to the brine treatment while the freshwater is sent to the post-treatment to achieve the drinkable standards.
The nature of the membranes does not allow ions to flow to the dilute zone even though they are attracted by the opposite pole ( Paul, 2004).

## 1.5 Other processes

Beside the three main processes, there are less spread ones. These processes are not widely used, because they are suitable only for specific application. Among these processes one of the most important is the manipulated osmosis desalination (MOD).
This process was developed to overcome the problem of the high osmotic pressure of the feed water that causes a greater applied pressure in order for separation to take place. The greatest innovation of this process is the presence of a carrier that has a greater osmotic pressure than the seawater. This causes a forward osmosis between the feed water and the carrier (Figure 1.12). Then this carrier, called draw solution, is pumped and sent to a reverse osmosis unit in which the water inside the solution is separated from the agent. Freshwater is collected and the draw solution is recycled (Gatto, 2012).

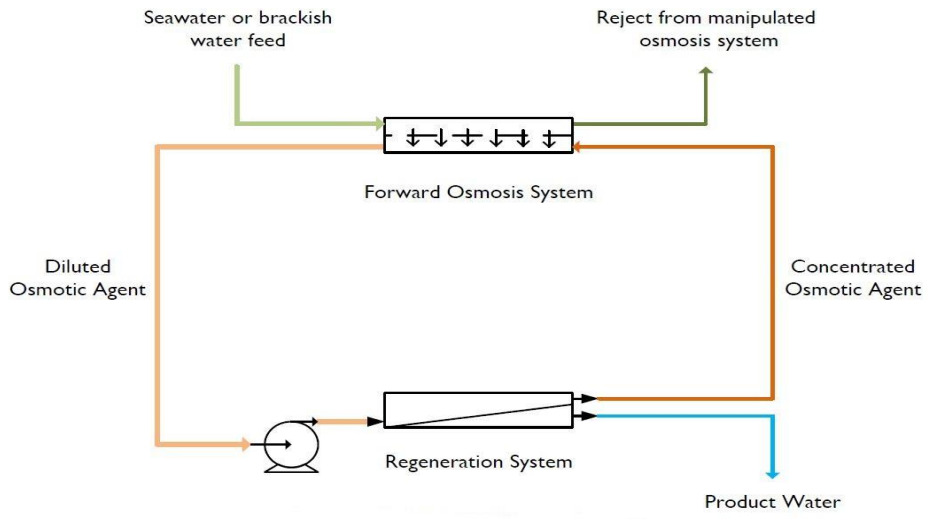


*Figure 1.12: Simplified MOD process diagram (Gatto, 2012)*

# Chapter 2

# Desalination by Humidification-Dehumidification

In this chapter a review of the process of water desalination by humidification-dehumidification is presented. The influence of the process parameter on the total amount of moisture and heat exchange is presented. In particular, a deeper analysis on heat and mass transfer characteristics is proposed and a review of the model developed for its prediction is showed.

## 2.1 Humidification- Dehumidification Process (HD)

The humidification-dehumidification (HD) desalination process is one of the secondary desalination processes but, despite this, it is very useful for places in which there is a low freshwater demand due to its low energy requirement and simplicity in both plant layout and management. Moreover, basics behind this process are very well known since air humidification and dehumidification naturally happens in the atmosphere during water cycle, as Figure 2.1 shows.

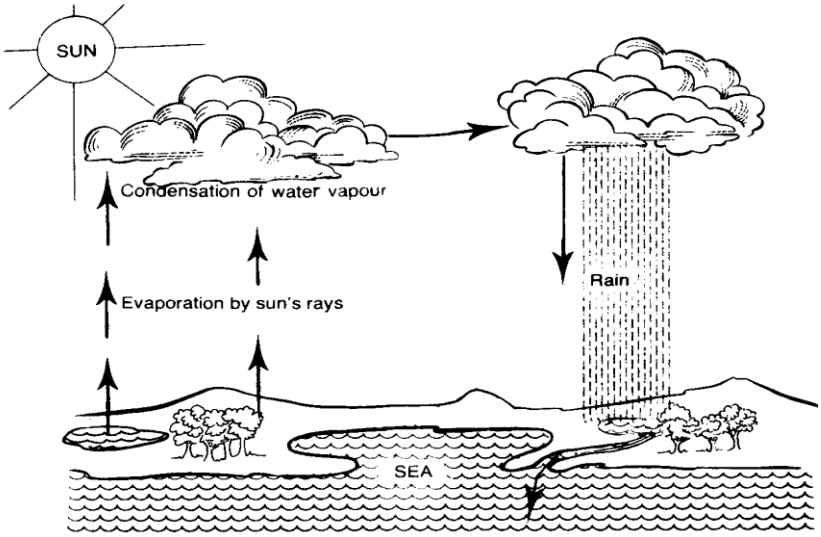


*Figure 2.1: cycle of water; the natural humidification and dehumidification process*

As it can be seen from Figure 2.2, the process is made of two columns, a water circulation system and an air one. Feed water drops down from the top of the column while an airflow goes up from the bottom. In this way fluids are put in direct contact and energy, usually provided by air flow, is transferred to the liquid. Consequently to this heat transfer, a certain amount of water vaporize and a mass transfer phenomenon to gas phase occurs. This vaporized water exits the column with air flow rate and it is sent to anther column in which this mixture is cooled. This second unit could be either a direct contact or a typical indirect contact heat exchanger, even if the direct one is more convenient. Freshwater is recovered simply decreasing the humid air temperature, and consequently decreasing the liquid solubility in air, allowing water condensation. At the end of the process, the dry gas could then be re-circulated (close process) or ejected from the process (open process). Studies carried out by Authors ( Bourouni, et al., 2001) show that recycling air improves the stability of the system, reduces the height of the column and decreases the operating costs. It is possible to recycle water too, but the salt concentration has to be measured carefully to ensure that its value lasts almost constant, otherwise some problems could appear, such as salt precipitation and reduction of heat and mass transfer efficiency. As about the first one, a salt precipitation brings to obstructions on the walls and bottom of the unit. The decrease of heat and mass transfer efficiency is due to the well-known effect that salt has on the boiling temperature of water.

Freshwater production depends on many parameters, such as air flow-rate and temperature, seawater temperature and flow-rate and coolant temperature and flow-rate (El-Agouz, 2010) (El-Agouz, et al., 2008) (Eslamimanesh, et al., 2009) (Hashemifard, et al., 2004). The latter mostly concerns the dehumidification step, in particular the water coolant temperature is important because the lower air temperature the higher is the amount of fresh water recovery. This is because decreasing air temperature decreases the solubility of water inside it, and so more water is condensed. Coolant flow rate is also important because increasing its value decreases the required time for the condensation, but a too high flow rate could have the opposite effect, not allowing heat exchange to occur and consequently losing some extracted water.

As far as the influence of the other parameters, they will be deeper analysed in paragraph §2.2.2.

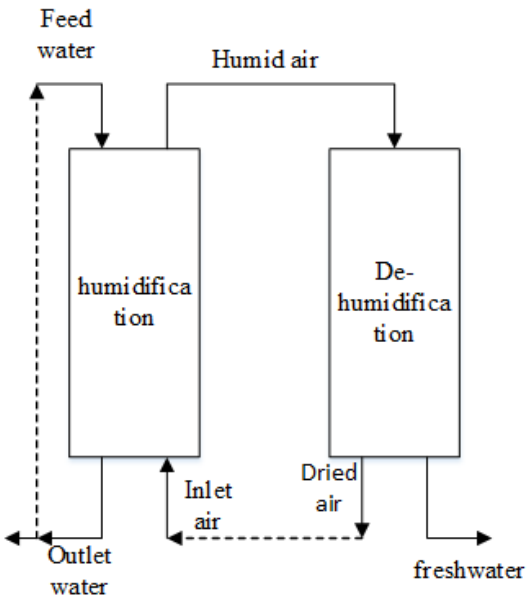


*Figure 2.2: layout of HD process*

As mentioned, one of the great advantages of HD process is that it does not need complex apparatus to work out, causing low capital and operating costs and simple maintenance. Moreover, heat transfer efficiency of this process is higher compared to classical thermal processes, because there are no walls between the two sides. Another point in favour of the HD process is that the pressure during the operation is the atmospheric one, and so the units are not put under mechanical solicitation. This permits both the use of common material and extends the life of the units. The only requirement for the material is that it has to be corrosion resistant, because the contact with seawater can bring unit deterioration.

In any case, it was observed by some authors that with the single stage process the amount of recovered water is 5-20% ( Bourouni, et al., 2001) of the total amount of feed water. To improve this quantity some authors studied the possibility to use a multistage process. They showed that the total amount of recovered water increased, but also increase the amount of energy required for the production, and energy/ Kg of water ratio lasts almost constant.

On the other hand, direct contact could lead to a contamination of the liquid solution. In fact, gas could diffuse inside the liquid and this could be a problem if gas can interact with the solution, but this diffusion has no dangerous effect on desalination purposes. Another disadvantage concerns how heat is provided to both the water and air. In fact, the process is competitive only if heat is available at low costs. To overcome the problem of energy source, many alternatives were developed. One of the most attractive is the

possibility to obtain the necessary heat directly from solar energy, especially in those areas that are poorly supplied with fuel or far from other energy sources.

Another possibility is to use geothermal water, which is hot but full of salts and minerals, as feed and energy source. This is a new and very interesting solution because heat necessary for water evaporation is given directly by the warm feed, without needing to pre-heat the inlet air. This water can also be used as an energy source for air pre-heating purposes, due to its high temperature that could reach 150 °C. Geothermal is also interesting because it allows to use desalination technique also in places where classical energy sources are expensive or solar energy is not so strong, such as the north part of France ( Bourouni, et al., 2001) ( Mahmoudi, et al., 2010).

A remarkable application is taking the necessary energy from industrial waste sources, such as exiting coolant fluid or exhaust gases. An example is found in India, where an HD plant was installed near an industry that uses seawater as coolant. Aside this example, many coastal industries use seawater as coolant and re-use this energy for other purpose instead of waste it could be an interesting way.

Also exhaust gases has a lot of energy (they could be at 400°C or more) that most of the time is wasted inside the atmosphere. A more smart solution, which is starting to appear in the last year with co-generation units, is the recovering of this heat and use of it.

Another possibility is to thermally couple the two processes, using the heat of dehumidification to pre-heat the air or the water feed. Of course this would not be enough due to energy losses, but at least it reduces the total amount of required energy and energy waste, increasing the energy efficiency of the system. An improvement of this process is the pressurized desalination process proposed by Vlachogiannis (Hashemifard, et al., 2004).

Columns suitable for humidification and dehumidification is the packed one, thanks to its great interfacial area, that allows great value of heat and mass transfer rate. Another used column is bubble column in which the air is flowed thanks to a sparger. Efficiency of the heat and mass transfer in this kind of column depends on the bubble size and size distribution. Another option, is to use a bubble column with water heater inside, this permits a further improvement to the heat transfer (El-Agouz, 2010) (El-Agouz, et al., 2008). The contact between the two phases can be made also with sieve column, but in this case capital costs increase prominently.

About the quality of the water coming out from the desalination process, it was proved that it is saturated with oxygen, but this problem could be easily overcome adding active carbon or dolomite.

## 2.2 Humidification side

The HD process consists of separated parts, the humidifier and the dehumidifier. In this work the attention is focused only on the first part: the humidifier. It consists of a column in which water flows down from the top in contact with an air counter-flow. This is the most common layout, but a co-current flow is used too. The advantage of using a direct contact exchange is that the heat and mass transfer is greater compared to an indirect heat exchanger and there are less heat transfer resistance. This causes an increase of fresh water production and a reduction of pressure drops and costs. One of the problems that can arise is the scale formation inside the column, especially into the packed ones. This problem, however, can be easily overcome by cleaning or discarding part of the brine to keep the salt concentration within controlled limits.
Desalination is only one of the many applications in which humidification process is used. Other applications are air conditioning systems, industrial processes prone to static and fire hazard, printing, textile paper products, containers of electronic facilities.

### *2.2.1 Thermodynamic of the process*

Thermodynamic plays an important role inside in the humidification process. In fact it manages the maximum amount of water that can be extracted from seawater at a specific inlet air temperature, which is linked with the saturation condition at the operating temperature. Due to air temperature decreases from the bottom to the top, it is necessary to see the exit temperature to understand the amount of water that can be extracted.
The amount of water inside the air is commonly called humidity and there are many way to express its value. The main are relative humidity (RH) and humidity ratio (HR). They are defined as:

$$RH = \frac{P_W}{P_S} \left[\frac{Pa}{Pa}\right]; \tag{2.1}$$

where $P_W$ is the partial pressure of water vapour (Pa) in the air and Ps is the saturation vapour partial pressure at the actual conditions (Pa).

$$HR = \frac{M_W}{M_A} \left[\frac{Kg\ of\ water}{Kg\ of\ dry\ air}\right]; \tag{2.2}$$

where $M_W$ is the mass of water inside the air (kg) and $M_A$ is the mass of the dry water (kg).
Using the ideal gas law, the 2.2 can be modified and expressed in terms of saturation pressure, the result is shown in Equation 2.3, in which $P_A$ is the pressure of the moist air, which can be approximated to the atmospheric one (Pa) without making a great mistake.

$$HR = 0.62198 \frac{P_W}{(P_A - P_W)} \left[\frac{\text{Kg of water}}{\text{Kg of dry air}}\right]. \quad (2.3)$$

The constant that appears after the substitution is simply the ratio between water and air molecular weight, necessary to convert the ideal gas law in terms of mass.
The maximum amount of water that can be found inside the air is obtained substituting $P_W$ with $P_S$ inside the 2.3, obtaining:

$$HR_S = 0.62198 \frac{P_S}{(P_A - P_S)} \left[\frac{Pa}{Pa}\right]. \quad (2.4)$$

This maximum amount of humidity can be predicted using a correlation for the saturated pressure of the water. For that purpose it is possible to use the Antoine Equation, reported below:

$$\ln \frac{P_S}{torr} = A - \frac{B}{\frac{T}{^\circ C} + C}. \quad (2.5)$$

where A, B, and C are the Antoine constants for the pure substance. In Table 2.1 are reported Antoine's constants for the pure water (Perry, et al., 2007).

*Table 2.1: Antoine coefficients for the pure water*

| **A** | **B** | **C** |
|---|---|---|
| 8,07131 | 1730,63 | 233,426 |

Figure 2.3 shows the behaviour of $HR_S$ calculated with Equation 2.5 using the coefficients reported in Table 2.1. Calculations are made under the hypothesis of atmospheric pressure for air and considering air temperature as that one exiting the humidification column.
As it can be been seen, the maximum amount of water increases with the temperature, but this amount is not so high, meaning that it will be needed a great amount of air to extract a remarkable amount of water.

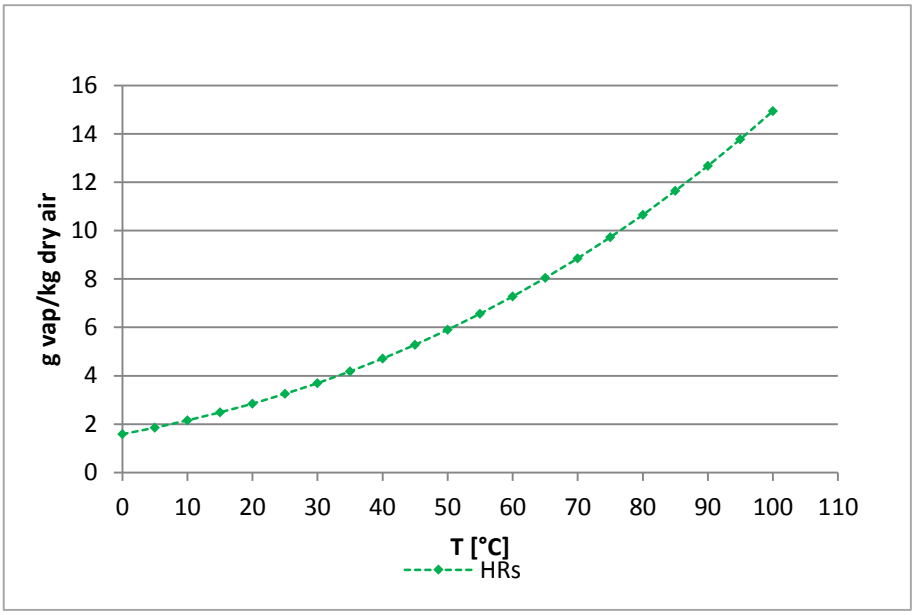


*Figure 2.3: HRs calculated with the Antoine equation*

## 2.2.2 Process parameters

To understand the behaviour of the system it is necessary to analyse which the influence of the main parameters is. Other studies were carried out in the past years on this process, and a review of the results is proposed here.

### 2.2.2.1 Air and water temperature

The air inlet temperature has an important role in the humidification process. In fact it is largely shown that increasing the inlet air temperature increases the amount of water extracted during the process.

There are two reasons why the total amount of extract water is higher if the inlet air temperature is increased. The first reason is a thermodynamic one; in fact, as shown before, the maximum amount of water increases with the temperature, and so a greater amount of water can be extracted. The second reason concerns the heat and mass transfer. Increasing the air temperature increases the driving force of the system, which is the temperature gradient. This causes a greater energy flux to the liquid and consequently it is observed an increase of the water evaporation rate. On the previous work, the analysed range of the inlet air temperature is between 30- 90°C (El-Agouz, 2010).

The amount of evaporation rate is influenced by the water temperature too. This is because the lower the water temperature, the higher the amount of energy spent as latent heat. The same Authors that analyse the influence of the air inlet analyse the water temperature influence and they showed that an increase of the inlet temperature (at a

constant air temperature) increases the amount of extracted water. The range analysed for the water temperature was similar to that used for water ( Bourouni, et al., 2001) (El-Agouz, 2010) (El-Agouz, et al., 2008) (Eslamimanesh, et al., 2009) (Hermosilo, et al., 2012).

The two parameters are not completely independent, in fact it was shown that the higher is the temperature of water, the lower air temperature is necessary and vice-versa.

Starting from this remark, two different way of doing emerged. Some authors sustain that it is more convenient increase the water temperature because evaporation needs less time. Other authors instead sustain that if water temperature is increased, salt solubility increases too, and this causes problems to the desalination process. This problem does not occur if air is heated instead of water, but the amount of latent heat available for the process is lower; unless the air temperature is kept high enough to increase the driving force. (Boehm, 1997)

#### 2.2.2.2 Air and water flow rate

Other important parameters are both water and air flow-rate. An increase of airflow rate increases the amount of extracted water thanks to a greater available surface. A common gas velocity range is 2.5-7.5 m/s (El-Agouz, et al., 2008), but this value strongly depends on the type of column used for the experiments.

As far as liquid flow-rate, it is shown that increasing its value increases the performances of the process. This increase has a maximum value, beyond which the performance of the humidifier decreases. This value is determined by a compromise between the increase of heat transfer due to an increase of the flow-rate and a decrease of the residence time of the water in the humidifier. If the residence time is not enough the heat and mass transfer cannot occur, and the process performance decay. It was also shown that this optimum value of the water flow-rate depends on the temperature of the fluids.

Sometimes it is preferred to analyse the influence of the water to air ratio instead of the single flow rates. It is proved that increasing this ratio the amount of fresh water produced decreases (Eslamimanesh, et al., 2009). This is because a great amount of available energy is lost as sensible heat instead of being used as latent heat for evaporation.

## 2.3 Heat and Mass Transfer

The humidification process involves both a heat and mass transfer, which can be analysed from the direct contact heat exchangers theory. These kind of exchangers have been largely used for many years and the most known and studied purposes are evaporative cooling towers and concentration processes, which show a lot of advantages compared to their counterpart, the indirect heat exchangers. First, there is no wall between the two

fluids; this brings to an increase of the heat and mass transfer coefficient and a reduction of thermal resistances inside the system and consequently an increase of the process efficiency. Moreover, the unit necessary for the process is made of simple columns, at the limit of a pipe full of water, with a decrease of capital and maintenance costs.
Direct contact heat exchangers have their main application in processes involving a phase change, evaporation and condensation, and the theory for both cases is almost the same. All the parameters affecting these two phenomena have been deeply studied for many application, but any study was found regarding humidification inside bubble column.

### 2.3.1 General description

In Figure 2.4 it is shown a simplified scheme of the process of heat and mass transfer that occurs on a bubble surface.

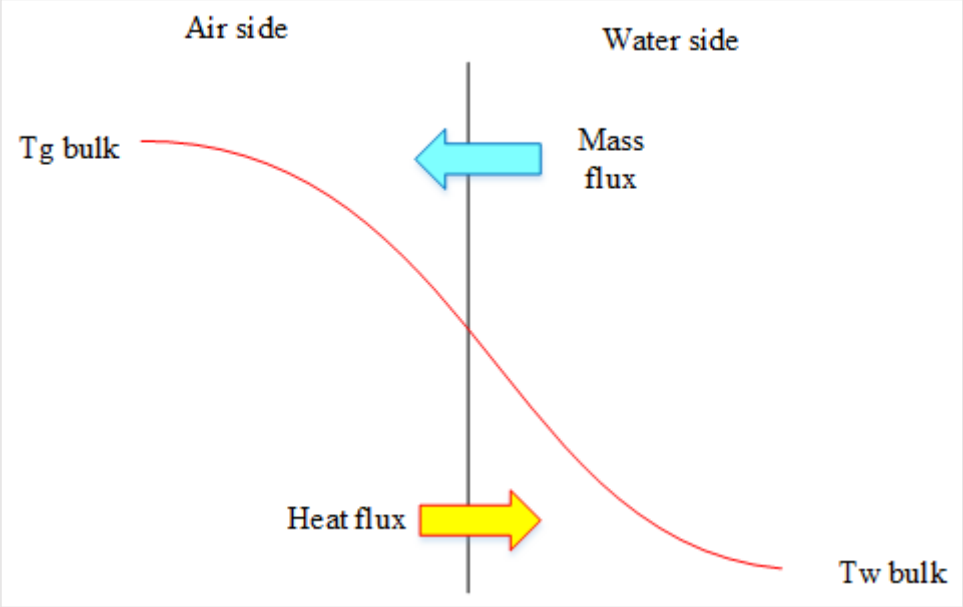


*Figure 2.4: simplified scheme of the heat and mass transfer*

System can be divided in three different regions: gas side, interface and liquid side. In each zone phenomena of heat and mass transfer occur, but with different mechanisms. In the gas side the heat transfer from inside the bubbles to bubbles surface is difficult to express because its formulation strongly depends on the motion inside the bubbles. If there is no air circulation, the phenomenon can be described as a pure diffusion, but if there is a recirculation of air, the governing phenomenon is the convection, so it is more useful to define the phenomenon with natural convection equations. The heat flux from the surface to the bulk of the liquid can be described with both convection and diffusion theory, it depends on the liquid recirculation inside the column. The place where heat

exchange take place is the surface between the two phases and, in this area, heat can be exchanged both as latent or sensible heat, depending on the fluids temperature.
The higher is liquid temperature, the higher is the amount of heat used as latent one, but in this case the driving force of the process is lower and there is less heat flux to the liquid.
Coupled with the heat transfer there is a mass transfer, which takes place mainly from the surface to the bulk of the gas, but it is possible to find a vapour flux from the bulk of the liquid to the surface if the temperature is high enough to allow the evaporation to take place inside the bulk liquid.
As about the mass transfer, the equation governing the motion from the surface to the inlet of the bubble depends again on the regime inside the bubble, if there is convection the referential equation are those of convection theory, otherwise the diffusion is the governing phenomenon.
The real amount of extracted water is far from the maximum amount given by the thermodynamic, but an estimation of it is necessary in order to have a preliminary idea of the performance of the process. The dimensionless number that could be helpful to this purpose is the Jacob number, which, coupled with the material balance, given the following relation:

$$M_V \leq M_L \frac{Ja_L}{1+ Ja_V} \tag{2.6}$$

Where $J_{aL}$ and $J_{aV}$ are the previous mentioned Jacob number of the liquid and vapour phase respectively, and they are defined as write in Equations 2.7 and 2.8 (Boehm, 1997):

$$Ja_L = \frac{C_{PL}(T_I - T_0)}{\lambda}; \tag{2.7}$$

$$Ja_V = \frac{C_{PV}(T_{amb} - T_I)}{\lambda}. \tag{2.8}$$

In the humidification process, most of the time $T_I$ (the temperature at the interface between the two phases) can approximated with $T^{sat}$ (saturation temperature). Moreover, this number, for this kind of processes, is very small: it means that it is necessary a greater amount of gas to evaporate a little amount of water. This theoretical investigation has a confirmation in the fact that the humidification process efficiency is very low, and it is necessary to have an air over water ratio very high to obtain a significant amount of water in the outside gas stream.

## *2.3.2 Role of the bubble surface*

The main exchange occurs at the bubbles' interface, it is clear that interface plays an important role in this process, and so it is very important to understand how its value and properties are influenced by system parameter and obtaining a good estimation of the total available area. The most influent parameters are reported in the following paragraphs.

### 2.3.2.1 Gas velocity

The interfacial area is strictly linked to bubbling regime, which strongly depends on the gas superficial velocity. Bubbling flow inside the column can be categorized in two different bubbling regimes: homogeneous and heterogeneous, and an example of them is showed in Figure 2.5.

Homogeneous regime appears at low gas velocity and it is characterized by small and uniform bubble size. The ascending trajectory is almost vertical and there are no interactions among the bubbles. It means that breakage and coalescence phenomena do not occur. Bubble size and gas holdup strongly depends on the type and design of the sparger, as well as the physical properties of the gas-liquid system.

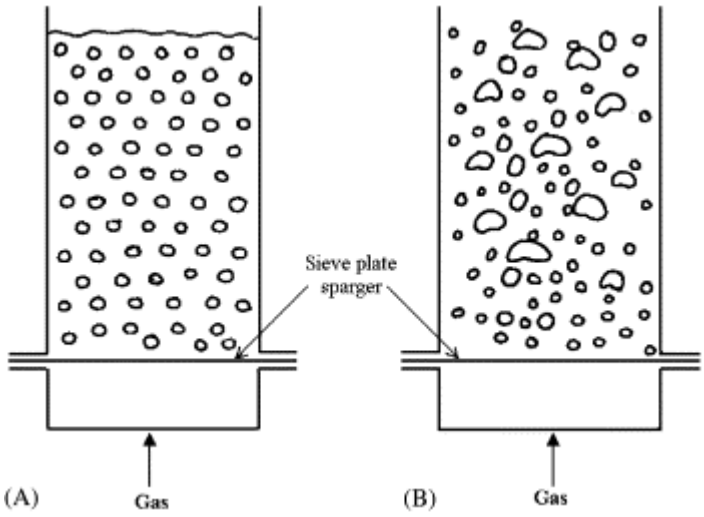


*Figure 2.5: examples of homogeneous and heterogeneous bubbling regimes (Boehm, 1997)*

Increasing gas velocity, the size of the bubbles increases while the distance among them decrease. This causes the rising of breakage and coalescence phenomena, which makes the size and the shape of the bubbles very different inside the column. These events occur when the bubbling regime is heterogeneous, which is the industrially used one, because of the great turbulence generated by the ascending bubbles. In this regime, the trajectory of ascending bubbles becomes irregular, causing both a liquid mixing and the gas holdup

is no more constant during the column length, but a parabolic holdup distribution appears, with a maximum in the centre of the column. Liquid recirculation is important because it improves the heat and mass transfer of the process. In this regime the sparger loses its influence upon the bubble size and their distribution, due to breakage and coalescence phenomena.

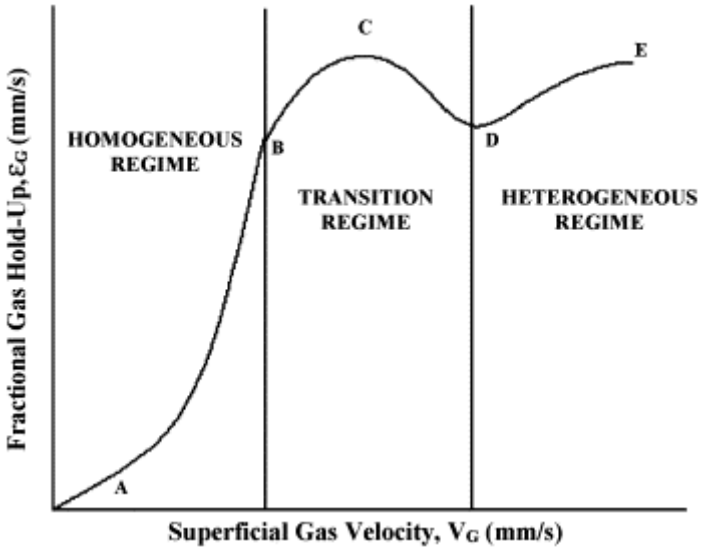


*Figure 2.6: transition among bubbling regimes (Boehm, 1997)*

Transition between regimes is not a sudden event and, under some hypothesis, it can be predicted. Figure 2.6 shows the characteristic behaviour of the transitional regime and, in particular, its effect on the gas holdup. As it can be seen, this transition shows a particular behaviour; in fact, after an almost linear correlation in the homogeneous zone, in the transition zone gas hold up reaches a maximum, and then it decreases until the heterogeneous regime is well developed and then it started to increase, again with a linear behaviour.

Other Authors studied also the effect of gas velocity both on the amount of extracted water and transient time of the process. They founded that an increase in the air velocity increases the amount of evaporated water and reduced the transient time of the process (Riberio Jr., et al., 2004).

### 2.3.2.2 Gas holdup

Another important parameter is, as mentioned before, the gas holdup, which, in its simplest definition, is defined as the gas volume fraction in the system:

$$\varepsilon = \frac{H_b - H_0}{H_b}, \tag{2.9}$$

where ε is the gas holdup, $H_b$ (m) is the boiling height, and $H_0$ (m) is the initial height of the liquid. Factors affecting ε are both linked with column structure and fluid characteristics. Formers are column diameter and sparger characteristics. In particular the greater the diameter is, the lower is the gas holdup. As about sparger, it is very important because it influences both superficial gas velocity and bubble size, an increase of gas velocity or a low mean bubble diameter brings to a higher ε (Boehm, 1997).
Beside these factors there are some linked with fluids characteristics, such as liquid molecular weight or solid suspended inside it. Other important factor is gas temperature, which influence gas viscosity. In particular, this aspect is even more important in non-isothermal column (like humidification), because the high change of air temperature brings to a lower gas holdup compared to the isothermal case.
Non-isothermal column are a more complicated case, because mass and heat transfer phenomena occur, and they affect its value. In particular, heat transfer affect gas temperature, which affects gas density; while mass transfer increases ε value because there is a change of mass in the gas side.

#### 2.3.2.3 Bubble size and size distribution

It was mentioned many times about the size and size distribution of the bubbles. There are two essential parameters for estimating the superficial area, place where the heat and mass transfer take place. The difficulty of this operation is that both distribution and size change during the column, especially for the non-isothermal one. This change occurs because of coalescence and breakage, mass transfer and temperature change.
The latter is important because the change of the temperature of the gas inside the column causes a variation of the molar volume of the gas. As about the mass transfer, due to the low efficiency linked to the process, it is not relevant as the previous. Other important phenomena are breakage and coalescence. These phenomena occur in different way along the column. Beside the sparger they are not so relevant, because the trajectory is almost linear but, ascending the column the trajectory can change and these phenomena can occur more frequently.
It is clear that bubble sizes change with the operating condition, and finding the optimal condition is not simple, because there are many variables in the system influencing this parameter.
Due to the complexity of the system, bubble size and size distribution in not easily predictable, and only few approximated and limited model were developed. The approach commonly adopted is a statistic approach. Basing on a finite number of size and distribution bubbles picture of the column a statistical distribution and a mean diameter is obtained; in particular, diameter is usually obtained first recording an experimental

running with special cameras, and then measuring pictured bubbles diameter and statistically analysing obtained data.

#### 2.3.2.4 Sparger

Another important part that must be taken into account is the importance of the sparger, not only for its primary function for bubble formation, but also for its contribution to heat transfer. It is in fact shown that an important amount of heat is transferred to the liquid by the sparger surface and it is not possible to ignore this phenomenon, especially in those systems in which feed water has not a continuous flow. If this heat is neglected, there is the risk of mistake in the heat transfer modelling, in particular it can lead to the conclusion that the system takes some heat from the surrounding, which is not true. Sparger has also a great importance for bubble diameter and column hydrodynamic; greater is the diameter lower in the velocity range in which homogeneous regime takes place because mean bubble diameter is higher and coalescence and breakage phenomena have more probability to occur (Riberio Jr., et al., 2004).

## 2.4 Heat and mass transfer modelling

From the previous analysis, it is clear that the all the parameters have an important role in the optimization of the process, and the dependences that occur among them make the process understanding more complicated. In this situation, an important role is played by the modelling of the process, in particular of heat and mass transfer and its reliance on the process variable. The published articles regarding bubble column modelling deal with isothermal column, in which only mass transfer occurs, while models regarding both heat and mass transfer have been published too, but they regard mostly packed column.
In any case, the proposed models are developed starting from mass and energy balance, sometimes written in differential terms other in global one, and the more complex one are written in order to analyse also the transient period.
Eslamimanesh *et al* (Eslamimanesh, et al., 2009) proposed a model for packing column that, starting from the input data and packing type, is able to predict the exit air humidity using an overall mass and heat transfer coefficients obtained analysing the inlet profile temperature. A limit of this model is that it was developed for a specific type of packing and under some hypothesis: constant water density, constant transfer coefficients, and quasi steady-state.
X. Li *et al.* (Li, et al., 2013) developed a simple model able to predict condensation rate and temperature profile for a packed column using an overall heat transfer coefficient given by a correlation that is function of dimensionless number; coefficient of this correlation were found out by experimental data fitting.

Also Kypritzis and Karabelas (Kypritzis, et al., 2001) , starting from dimensionless number and fitting, developed a model for water evaporation in a packed column able to predict both heat and mass transfer. They used overall equations and, in particular, they divided heat in two parts, sensible and latent and dividing the column in many sections.
A model for bubble column was proposed by Mahood *& al* (Mahood, et al., 2013), but the analysed system was different because it deals with a three-phase heat exchanger. The peculiarity of this model is that it takes into account also effects due to friction with wall of the two fluids.
The model which is closest to this work is the one developed by Kang *et al.* (Kang, et al., 2002); they analysed temperature profile in a spray column considering also the radial component of bubble velocity. So, they solved continuity, momentum and energy equations together, obtaining good results as far as temperature profile prediction.

## 2.5 Other applications of humidification system

Desalination is only one of the purposes in which humidification technique is used, other interesting applications are energy recovery from waste gases and as pre-heat system for other desalination techniques, such as RO.
Great amount of energy can be recovered from exhausted gases or hot waste streams. This great amount of heat can be used both to heat and evaporate amount of fluids. Heated fluid can be used directly while the evaporated part could be condensate recovering the latent heat.
A new interesting application is use desalination as pre-treatment for RO systems. This is similar to the previous described energy recovery, but the used fluid is water and the evaporated part is condensed to obtain freshwater. The heated liquid part, instead, in sent to an RO unit. It could be a good alternative because a temperature increase allow also to a flux increase.

## 2.6 Aim of the work

The aim of this work is to investigate the heat transfer rate and its dependence on the main parameters of the process, such as air and water flow rate and air temperature. Starting from the experimental data, an experimental value of the heat transfer coefficient were calculated and then it was checked with existing correlations, in order to see if they are suitable for a coefficient prediction. At the end of this work, the best correlation were tested with a simple developed model, and an air temperature profile and the amount of extracted water were predicted.

It would be very important to obtain a realistic values prediction of these parameters because a good estimation of them could allow to save money and time.
This work is also important because two important issues of the last years can be coupled and solved together. One concerns the great amount of waste energy, coming from coolant cycles or combustion exhaust gases, which many industries have and that could be used to produce water at low costs. The other great problem is the water shortage in some regions; if freshwater can be produced by this simple and cheap technique; this could help to improve the amount of available freshwater in regions where other techniques are not suitable.

# Chapter 3

# Experimental Unit and Procedure

In this chapter, a description of the experimental set up is presented, highlighting the important characteristics of each unit.
The experimental procedure is then reported, together with and calculations for data analysis.

## 3.1 Experimental Unit

A schematic of the experimental unit is shown in Figure 3.1. Here the main components are: the column (reference 7 in Figure 3.1), the thermocouples (8, 18, 19, 20, and 21), the valves (5, 10, and 16), the pump (3), the flow (6, 9,) and pressure meters (4, 12, 13, 14, and 15), moisture meters (17), air heater (11) and feed tank (1).

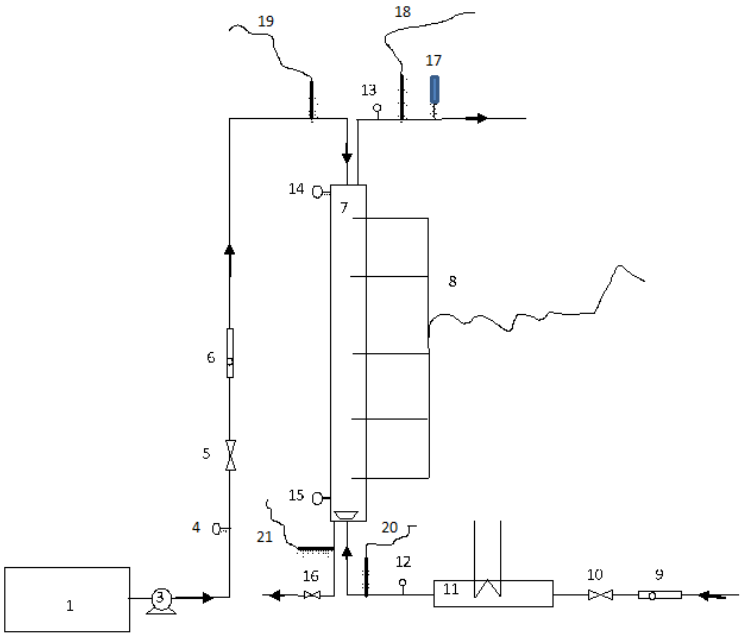


*Figure 3.1: schematic diagram of the column*

### 3.1.1 Column

This column, designed and built by University of Surrey, is represented in the picture of Figure 3.2a.

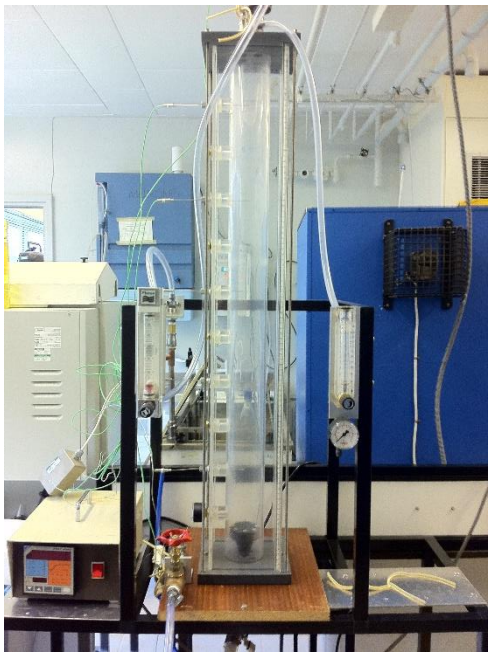

*Figure3.2a: picture of the experimental unit*

*Figure 3.2b: detail of the sparger*

It is composed by a Perspex cylinder inserted in a rectangular external jacket of the same material, which was designed to limit as much as possible heat losses and external influence on the heat exchange within the column. Perspex is an acrylic resin (Methylmethacrylate) produced by Perspex Distribution Ltd. It is water resistance, can be heated up to 60°C without problems and is a good thermal insulator.

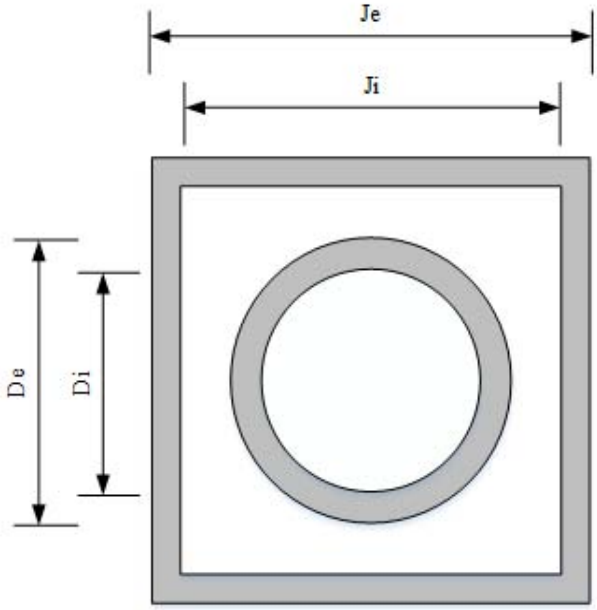


*Figure 3.3a: cross section of the column*

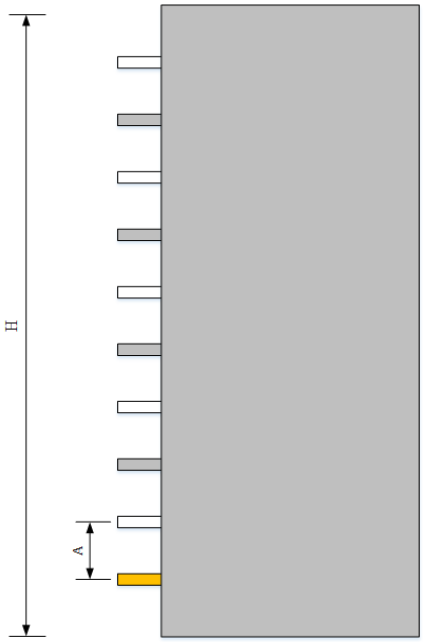


*Figure 3.3b: longitudinal section of the column*

The column dimensions are reported in Table 3.1, referring to the drawing in Figure 3.3a,b.

*Table 3.1: column specification*

| De [cm] | Di [cm] | Je [cm] | Ji [cm] | H [cm] | A [cm] |
|---|---|---|---|---|---|
| 8 | 7 | 14 | 12.8 | 99 | 9 |

On the column side there are 10 holes, each one 9 centimeters apart from the next (specify called A in Table 3.1). The first and the last holes have also distance A from the bottom and the top of the column respectively. Five of these holes, identified with white colour in Figure 3.3b, are used for the thermocouples. The grey ones were not used; while to the orange one (first from the bottom), a barometer was connected.

Figure 3.2b shows that at the bottom part a sparger is placed, which 6 cm high is. It has a truncated cone shape, and on its base there are 14 holes, each one 3 mm diameter.

The sparger and all the pipes are connected to the main column by two plates, which have also the function to close the column. Column is connected to the two plates thanks to 4 long screws, located on each corner of the plate (detail in Figure 3.2).

They dimensions are 18x18x1.3 cm and they are made of PVC, rigid and enough resistant to chemicals.

### 3.1.2 Flow meters

There are two volumetric flowmeters on this unit, one for the inlet water and one for the inlet air, those main characteristic are reported in Table 3.2.

*Table 3.2:flowmeters characteristics*

| **Type** | **Name** | **Range (L/min)** | **Accuracy** |
|---|---|---|---|
| **Air** | Platon NGXV | 6-50 | ±5% |
| **Water** | Ki FR4500 | 1-20 | ±3% |

### 3.1.3 Moisture meter

The moisture meter used is a *RS-1360 Digital Humidity/ Temperature meter*. As about the humidity measurement, instrument specifications are reported in Table 3.3.

*Table 3.3: moisture meter specification*

| **Measurement Range** | **Resolution** | **Accuracy (at 25°C)** | **Sensor Type** | **Response time (45% to 95%)** |
|---|---|---|---|---|
| 10%-95% RH | 0.1% RH | ±3% | Precision capacitance sensor | ≤ 3 min |

### 3.1.4 Pressure meter

Pressure measurements were carried out using barometers Model 111.12, produced by WIKA and distributed by RS (stock number RS 405 5571). They are 0-6 bar range pressure gauges with an accuracy of ±1.6 % (on full scale).

### 3.1.5 Thermocouples

K thermocouples were used, as they are inexpensive and ensure a wide range of applicability (-200-1350°C). K type thermocouples are made of Chromel (+) and Alumel (-). Typical sensitivity of this kind of thermocouples is 41 μV/°C.

Overall, nine thermocouples were used; five of them were located along the column, one was used for the air outlet temperature, one for the air outlet temperature, and the remaining two were used for water inlet and outlet temperature measurement. Except for the air inlet one, all the others were connected with the data logger. It is a USB TC-08, by Pico Technology, equipped with an eight inlet channels and can be connected to a laptop, to make easier the acquisition and data analysis.

### *3.1.6 Air heating system*

The heater used is a *RS Stock Nos. 200-2547*, whose specifications are reported in Table 3.4.

*Table 3.4: air heater characteristics*

| **Maximum temperature** | **Sheath material** | **Sheath end (hot)** | **T piece** | **Sheath end (cold)** | **Coil support** |
|---|---|---|---|---|---|
| 540 °C | Stainless steel | Stainless steel | Copper | NPT brass | Ceramic |

Air temperature was maintained to the desired value by a PID controller WEST 2050.

### *3.1.7 Pump and Tank*

The pump was a HPR 6/8 by Totton Pumps, which is a regenerative pump with run out flow rate of 5.5 L/min. It sucks water from a 145 L polypropylene tank, used as a storage for the feed to the main column, and made by Very Useful Products Ltd.

## 3.2 Air and water characteristics

In the experiments air and tap water were used. Air was provided by the University air supply system, at a temperature of 25°C and dry.
Water was supplied by the University system as well. The choice to use freshwater instead of sea or salt water is because this work is a preliminary analysis and characterization of the system behaviour, so a deeper and more complicated analysis will be done later, when the experimental setup will be used to investigate the effect of salt concentration on the heat and mass transfer.

## 3.3 Experimental Procedure

Before starting with the experimental work, the unit had to be installed and tested in order to find and fix problems and check the instruments. This test was useful also to understand the best conditions for the experimental runs: duration, air and water flowrate ranges and sampling time. The ranges investigated are reported in Table 3.5.

*Table 3.5: analysed experimental range*

| **Water flow rate** | **Air flow rate (at 25°C)** | **Air temperature** | **Experiment duration** |
|---|---|---|---|
| 2;3 L/min | 6-12 L/min, step 2L/min | 30-70 °C, step 5°C | 40 min |

Even if the pump was able to cover flow rate from 1 to 4 L/min, difficulties were observed to get a stable flow rate with the lower and upper values, so they were excluded.
The lower limit of the air flow is the one given by the air flow meter, while the upper one was decided looking at the column flooding condition. In fact, for higher values, the column flooded and water came out from the top wetting the moisture meter.
The air temperature range was decided looking at the connections thermal resistance, while experiment duration was set as 40 minutes to ensure steady state for all the parameter carried out.
The experiments have been performed according to the following procedure:

- air flux and temperature was set to the desired value. In order to guarantee that air temperature were the desired one, air flux were left flowing for 10 minutes before opening the air supply to the column;
- meanwhile air reaches the desired temperature, the column was filled with water, which were circulated in order to achieve uniform conditions. Between two experiments the column was emptied and then refilled, so that to avoid influence between subsequent runs,
- the air flux valve was open in order to start the air supply to the column. After that, temperature recording was started.
- the first humidity measurement was obtained after 30 seconds of column run; it was decided to operate in this way to give time to the moisture meter to reach a stable value
- the following moisture measures were taken every two minutes, until the end of the run.

The moisture meter output was in term of relative humidity, so the exact amount of water coming out with was determined converting this value to humidity ratio.
Relative humidity and humidity ratio are defined as reported in Equation 2.1 and 2.2; HR can be expressed in terms of pressure instead of mass, using the ideal gas law.
At saturation condition, water pressure can be calculated as water vapour pressure, while below saturation, it can be expressed as:

$$P_w = RH * P_S\ [Pa], \tag{3.1}$$

and Equation 2.3 becomes:

$$HR = 0.62198 \frac{\mathrm{RH} * \mathrm{P_S}}{(\mathrm{P_A} - \mathrm{RH} * \mathrm{P_S})} \left[\frac{\text{Kg of water}}{\text{Kg of dry air}}\right]. \tag{3.2}$$

All the graphs reported in Chapter 4 and 5 are expressed in terms of humidity ratio, which better indicates of the real amount of water extracted.

# Chapter 4

# Experimental Results and Discussion

In this chapter the experimental results are presented. The discussion is focused on showing the influence of process parameters on the temperature, the amount of the extracted water, the gas holdup and the column hydrodynamic. As about temperature and extracted water, the discussion is divided into steady state and dynamic analysis. At the end of the chapter a general summary of the results is presented.

## 4.1 Temperature distribution

### *4.1.1 Steady State*

A first analysis concerns the effects of parameters on outlet water temperature change.

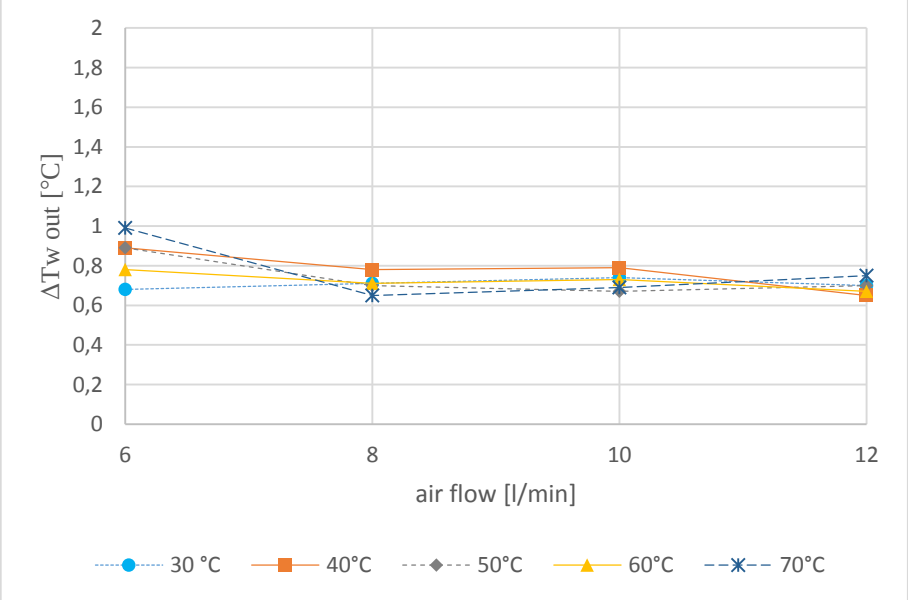


*Figure 4. 1: water temperature difference between outlet and inlet, flow rate 2 L/min, parametric in inlet air temperature*

As can be seen in Figure 4.1, the water outlet temperature is slightly affected by both air temperature and flow rate, and its increase is always lower than 1°C.

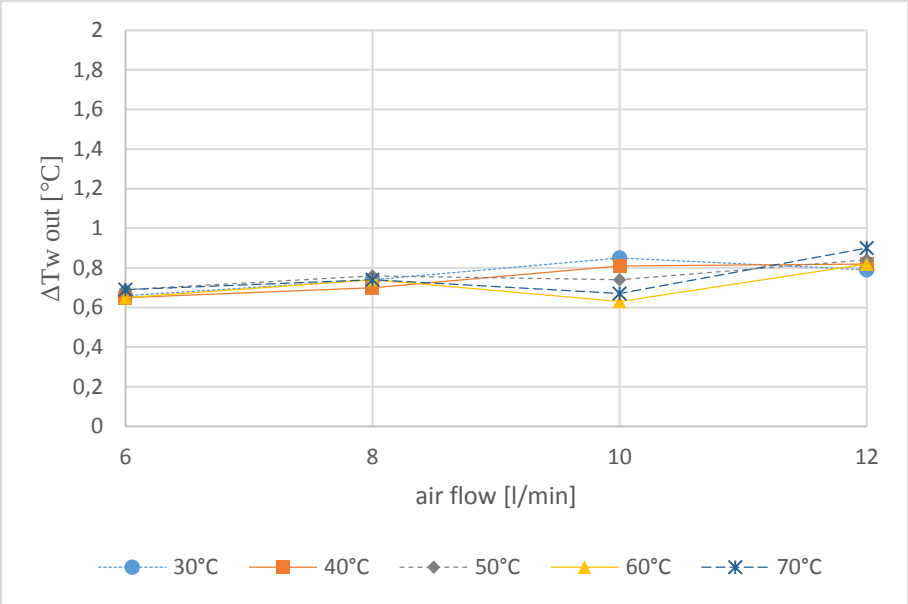


*Figure 4.2: water temperature difference between outlet and inlet, flow rate 3 L/min, parametric in inlet air temperature*

Figure 4.2 shows the water temperature rise for a water flow rate of 3 L/min. Also in this case the influence of both air temperature and flow rate are not appreciable, as the water temperature increase is always less than 1°C. The comparison of Figure 4.1 and 4.2 allow to have an idea of the influence of water flow rate on the temperature rise, showing also that water flow rate has no appreciable effects on this parameter. A reason to explain this behaviour is that the column is short, and this does not allow enough heat exchange to enhance water temperature. Another reason is the specific heat of water, compared with the low $C_P$ of air (4.18 against 1 kJ/kgK), which causes a large requirement of air to enhance water temperature.

Figure 4.3 shows the difference between inlet and outlet air temperature, for a water flow rate of 2 L/min. It can be seen that values increase with the increase of the inlet air temperature but, most importantly, they are almost constant with the air flow rate. This could mean that with all air flow rate the system is able to exchange all the available energy.

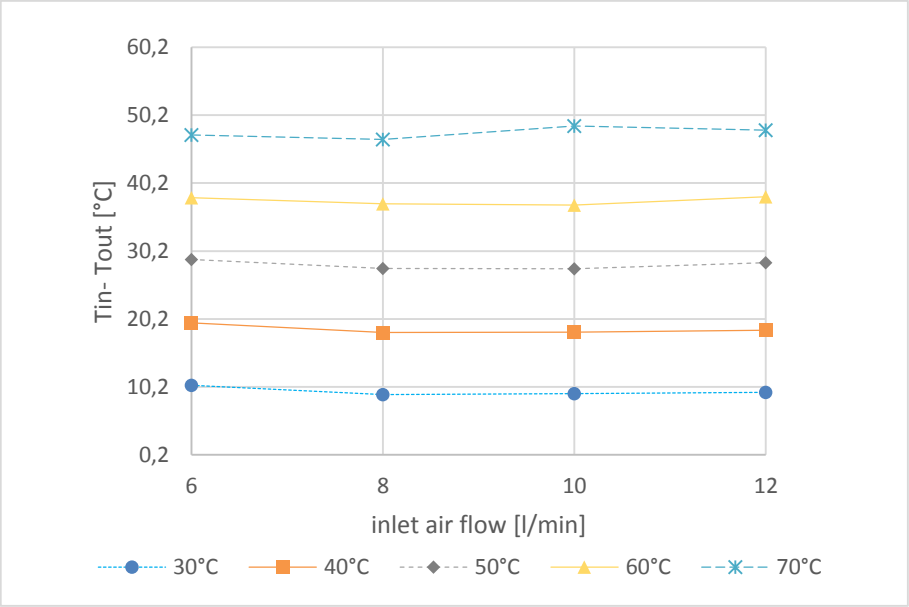


*Figure 4. 3: air inlet-outlet temperature difference, water flow 2L/min, parametric in inlet air temperature*

Figure 4.4 is similar to Figure 4.3, but for a water flow rate of 3 L/min. Like in the previous case, air flow rate has no significant influence on the parameter and the difference value is constant for all the condition considered, for a given inlet temperature.

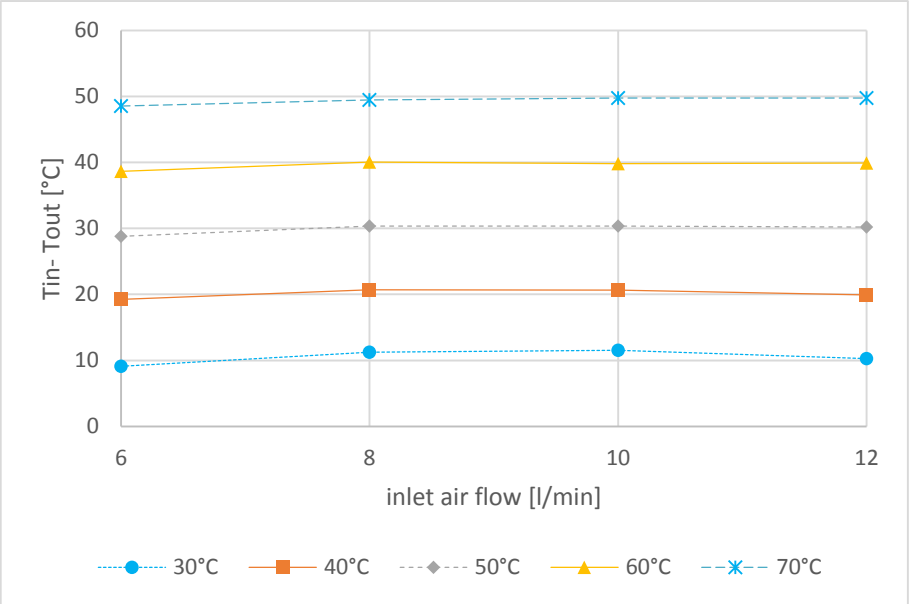


*Figure 4.4: air inlet-outlet temperature difference, water flow 3 L/min, parametric in inlet air temperature*

Figure 4.5a and 4.5b show the temperature difference at the top and bottom of the column between air and water streams. This is just one case (air flow of 10 L/min), because a similar behaviour was found for the others air flow rates.
It can be seen that the maximum difference, corresponding to a maximum driving force, is at the bottom of the column, where the air temperature is higher, and this driving force increases linearly with the air inlet temperature.

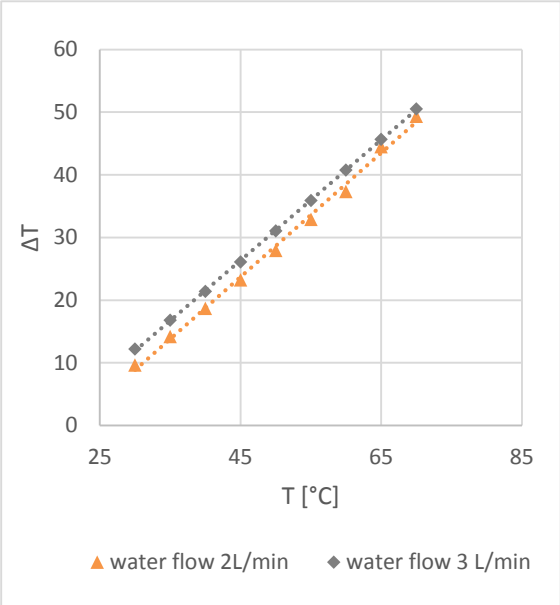


*Figure 4.5a: temperature difference between air and water at the bottom of the column, parametric in water flow rate*

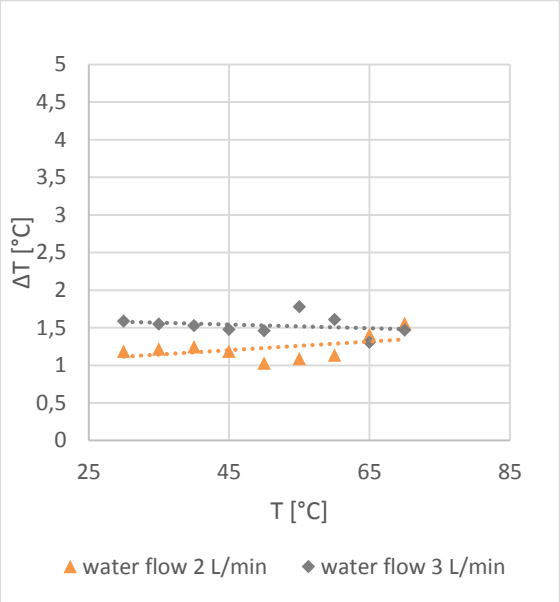


*Figure 4.5b: temperature difference between air and water at the top of the column, parametric in water flow rate*

Figure 4.5b shows that there is no influence of both air temperature and flow rate on this parameter, as its value is nearly constant along all the range considered. It could mean that the efficiency of the heat transfer is very high, because air exit temperature is very close to the water inlet one. Even though all the available heat is transferred, water temperature does not rise; this is so because a much larger flow rate of air would be needed to enhance water temperature.

### *4.1.2 Transient Period*

Another important aspect is the analysis of the temperature profile inside the column during experimental runs. Temperature profile is important in order to understand which part of the column is relevant for the exchange, and to see if all the column length is useful for it.
As meaningful example, only one of the best experiment in term of extracted water will be reported, details are reported in Table 4.1.

*Table 4.1: detail of specifications for the selected experiment*

| AIR FLOW [L/min] | WATER FLOW [L/min] | AIR TEMPERATURE [°C] |
|---|---|---|
| **10** | 2 | 45 |

Figure 4.6 shows the trend of the two outlets (air and water) and water inlet temperature with time. Even if there is a little increase of these temperatures, the most important thing that is that, except for the first times (when air temperature decreases rapidly), the difference among them remains for all the experimental time.

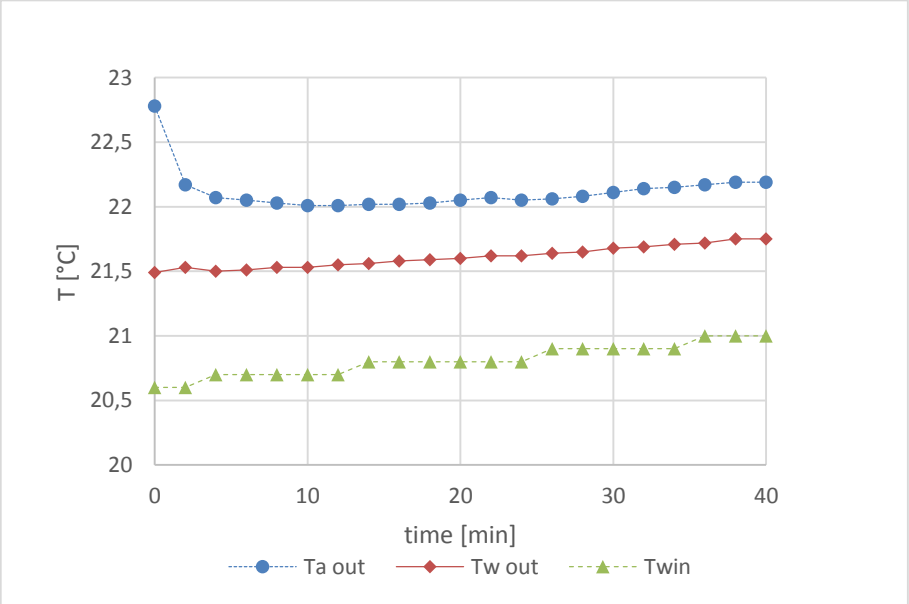


*Figure 4.6: temperature distribution with time for air outlet temperature and water inlet and outlet temperature*

Figure 4.7 shows the air temperature reduction for the selected experiment in terms of inlet minus outlet values. It can be seen that the difference between the two temperatures increases rapidly, to set at an almost constant value. This means that at the beginning the heat exchange is scarce, but it reaches and maintains its maximum value quickly. The final temperature different reduction is probably due to the fact that also water temperature increased, as previously noticed in Figure 4.6.

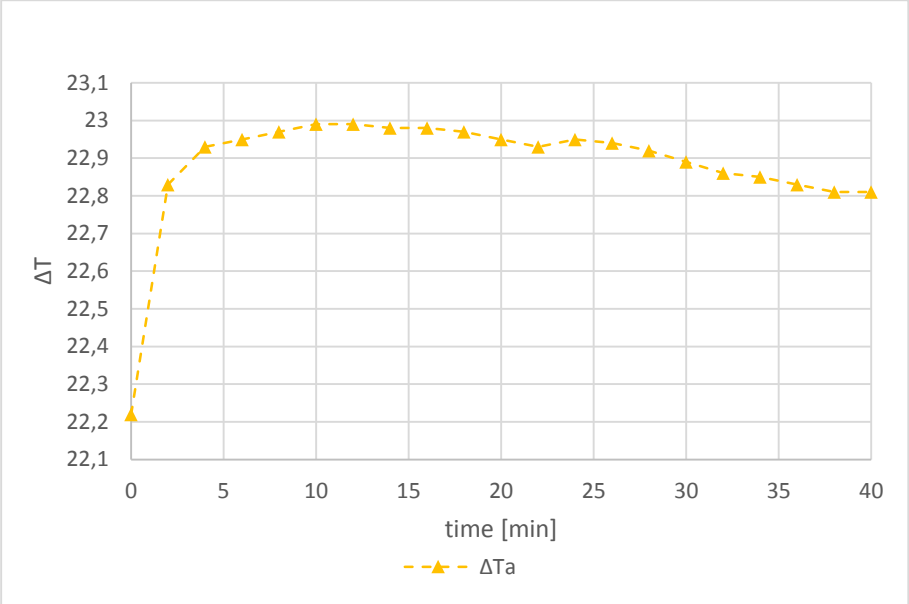


*Figure 4.7: air temperature difference during time*

The phenomenon in Figure 4.6 is better understood from Figure 4.8, where the difference between air and water at the top of the column is reported. This difference decreases quickly with time, to reach a steady state value that lasts for all the experiment.

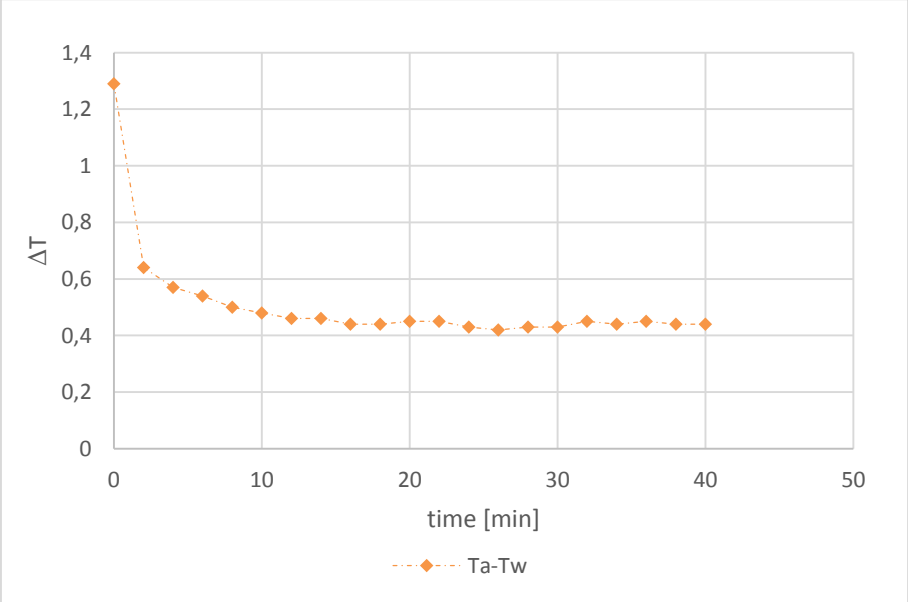


*Figure 4.8: air-water outlet temperature difference with time*

As about the water temperature profile distribution along the column, Figure 4.9 shows the internal temperature profiles along with time. First, the temperature difference between the first thermocouple (Ch. 2) and the last one (Ch. 6) is very low, less than

0.5 °C. Second, this temperature difference remains constant with time, even if all the temperatures has a general increase, mostly due to the increase of the inlet water temperature (compare with Figure 4.6).

It is also interesting seeing how the water temperature profile is at a given time. All the profiles are similar, so the situation at last the measurement, shown in Figure 4.10 was represented.

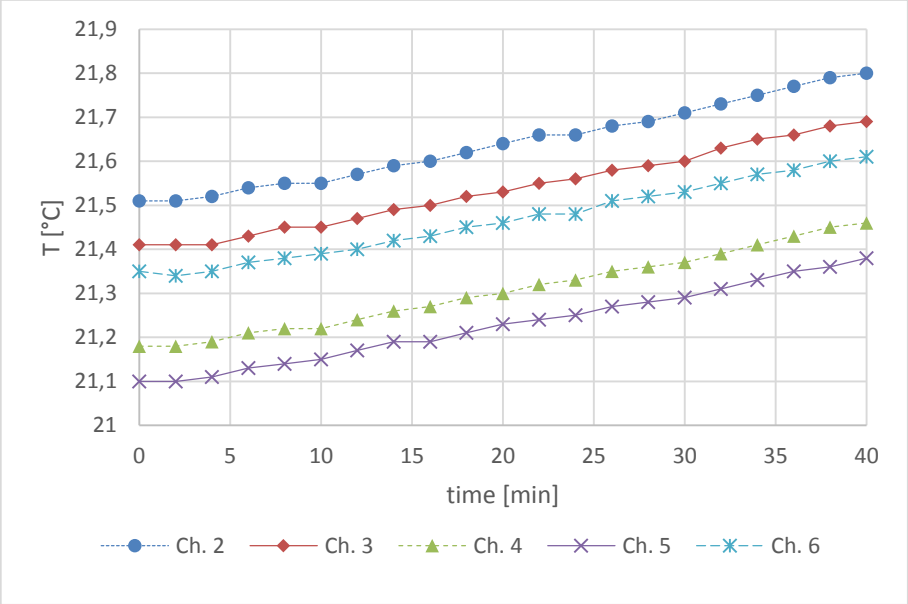


*Figure 4.9: temperature distribution inside the column with time*

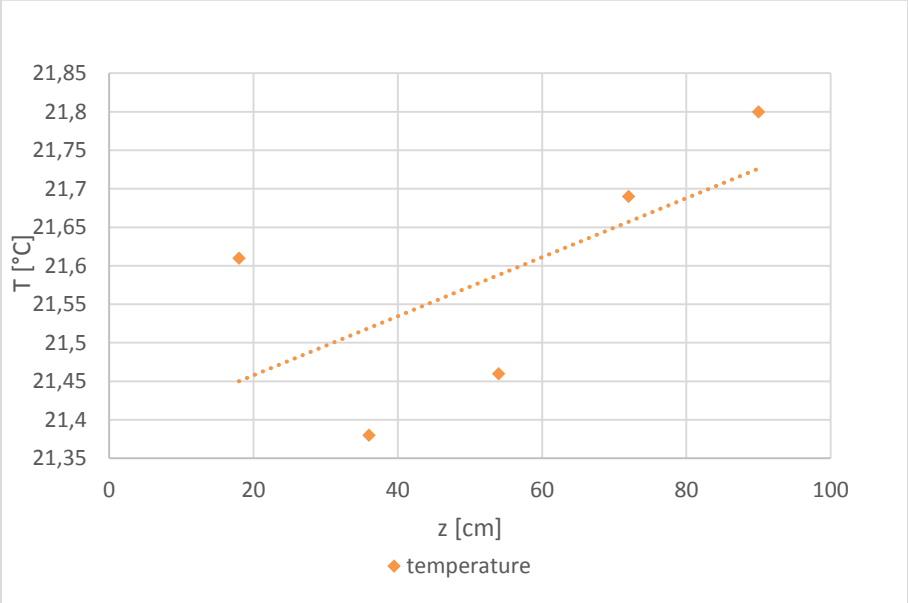


*Figure 4.10: temperature profile distribution along the column at the final time measurement*

The temperature profile in Figure 4.10 shows that water temperature change along the column is very small and the resulting trend is affected by measurement errors. Nevertheless, the behaviour is not unreal, because it is known that heat of vaporization is given also by water and it could explain why water temperature decreases from the top to the bottom (Eslamimanesh, et al., 2009). The final temperature increase could be explained considering the heat transferred by the sparger, as suggested by Riberio (Riberio Jr., et al., 2004).
It was also seen that a temperature difference of ±1°C on water inlet temperature influences also the outlet air temperatures (± 1°C), and consequently the amount of extracted water. This aspect was not taken into account in this work, so an interesting development could be to analyse the influence of water temperature.

## 4.2 Extracted water

### *4.2.1 Steady State*

One of the most important parameter is the amount of extracted water from the top of the column. Figure 4.11 and 4.12 show the influence of air flow rate and temperature on the amount of extracted water, for each water flow rate.

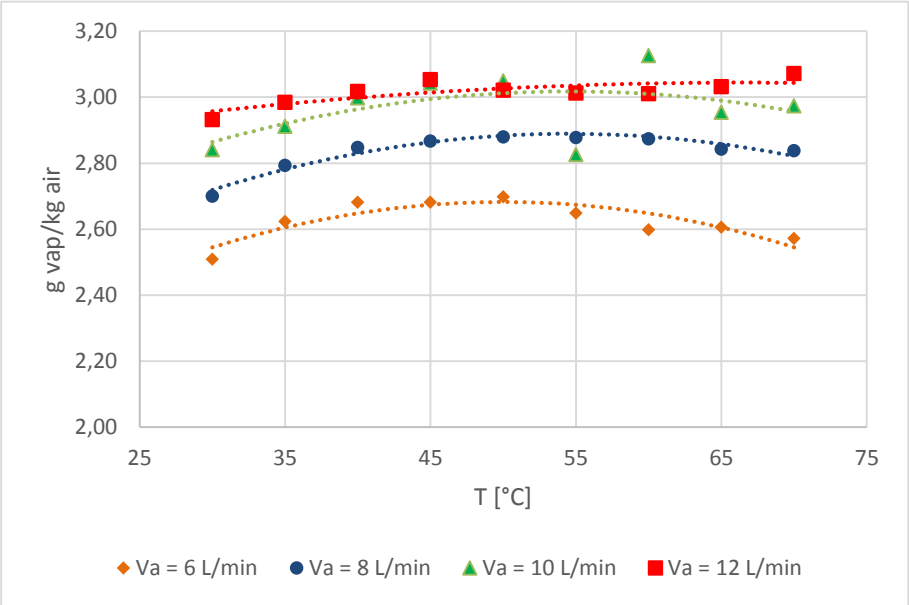


*Figure 4.11: amount of extracted water, water flow 2 L/min, parametric in inlet air flow rate*

In particular, Figure 4.11 shows an influence of both air temperature and flow rate. It is confirmed that an increase of flow rate leads to a larger amount of extracted water

(Riberio Jr., et al., 2004) (El-Agouz, 2010). Instead, the extracted water displays a maximum when plotted against temperature.

It can also be noticed that with air flow rates of 10 and 12 L/min the amount of extracted water is nearly the same. The obtained trend does not surprise, because the same behaviour was found also in other studies (Hashemifard, et al., 2004).

From Figure 4.12, it is seen that there is no influence of air flow rates, as the amount of extracted water can be considered constant for all of them. Their difference with Figure 4.11 leads to the conclusion that water flow rate plays an important role on the amount of extracted water. In order to understand if there is a relationship among water flow rate, air flow rate and the amount of extracted water, the air to water ratios are taken into account instead of the absolute values, as Eslamimanesh suggested in his work (Eslamimanesh, et al., 2009). This means that for water flow rate of 2 L/min the analysed ratios were 3, 4, 5 and 6, while for water flow rate of 3 L/min the analysed ratios were 2, 2.6, 3.3 and 4.

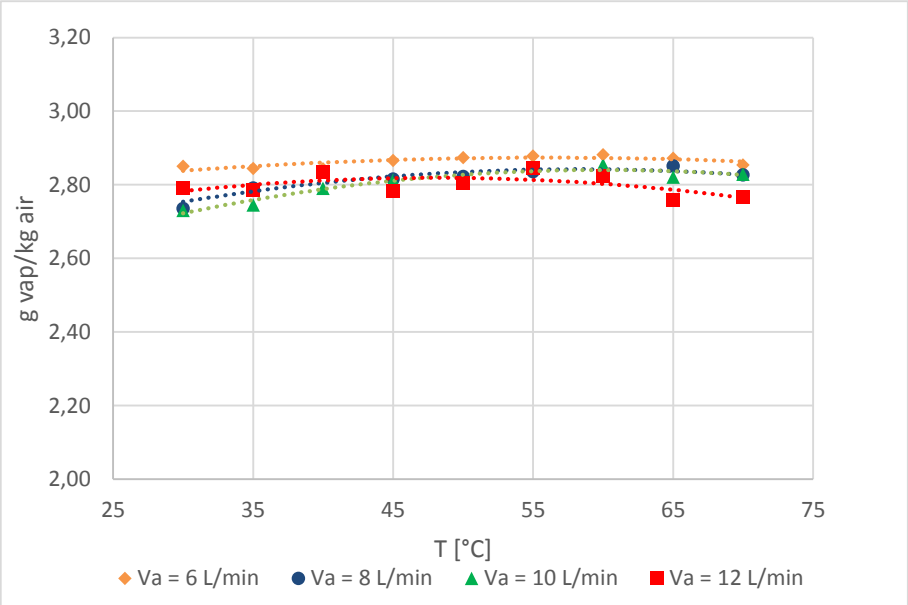


*Figure 4.12: amount of extracted water, water flow 3 L/mi inlet air, parametric in inlet air flow rate*

Figure 4.13 shows the comparison of cases 3 and 4 with 2 L/min and 3.3 and 4 with 3 L/min. It shows that for values of air to water equal to 4, the amount of extracted water is nearly constant, while a difference is noticeable between air to water ratios 3 and 3.3. These data are not enough to say if the air to water ratio can be taken as the relevant parameter. A future development of this work could be the analysis of same air to water ratios obtained under different condition.

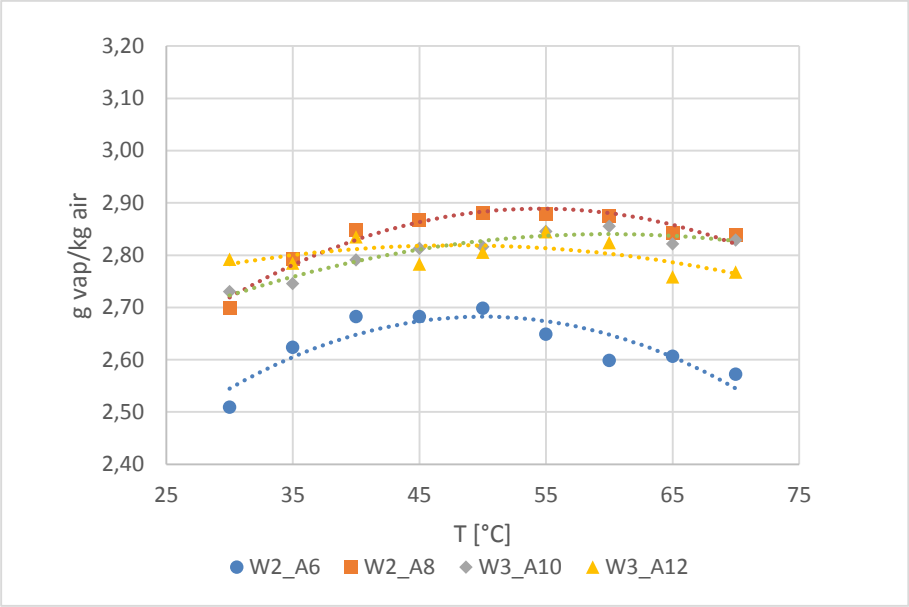


*Figure 4.13: comparison among different air to water ratios; W indicates the amount of water flow rate, while A the amount of air one*

Another important aspect arises from Figure 4.11, which is the effect of temperature on the amount of extracted water. This reaches a maximum, which is always between 50 and 60°C. Also Figure 4.12 shows this behaviour in the same temperature range, even though this effect is less marked.

Figure 4.14.a, 4.14.b, 4.15a, 4.15b compare the behaviour of the two water flow rates at constant air flow. Looking at the four graphs, it can be concluded that at low air flow rate it is more convenient having a higher water flow rate; while a lower water flow rate is the best choice if the air flow increases.

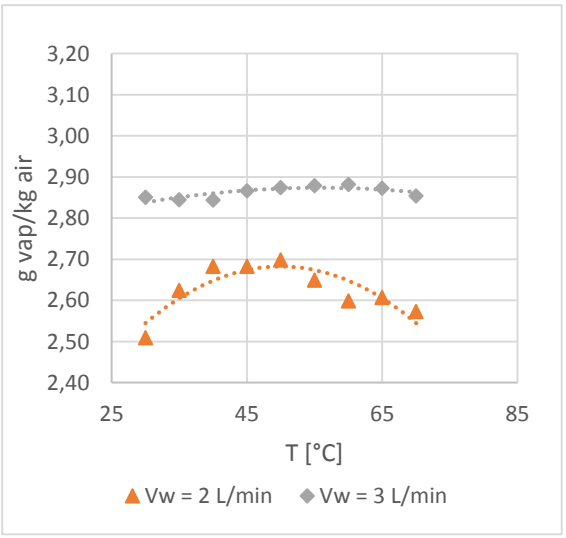


*Figure 4.14a: comparison of different water flow at constant air flow of 6 L/min, parametric in inlet water flow rate*

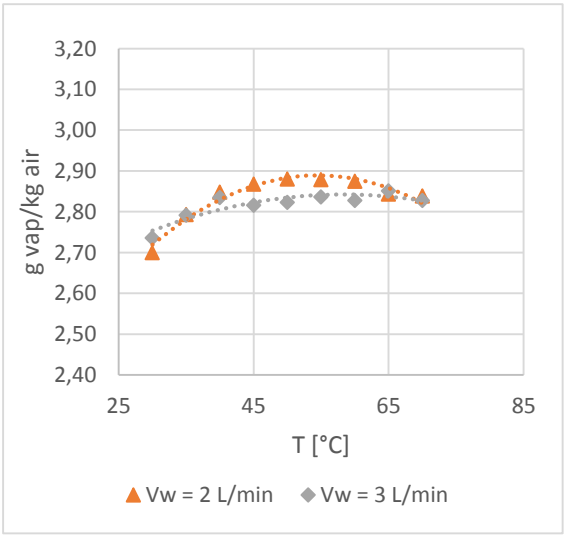


*Figure 4.14b: comparison of different water flow at constant air flow of 8 L/min, parametric in inlet water flow rate*

In fact, in Figure 4.14a can be noticed that the amount of extracted water is higher with a water flow rate of 3 L/min with all the inlet air temperature. Instead, with higher air flow rates (10 and 12 L/min, Figures 4.15a and b) the amount of evaporated water is higher with a lower water flow rate.

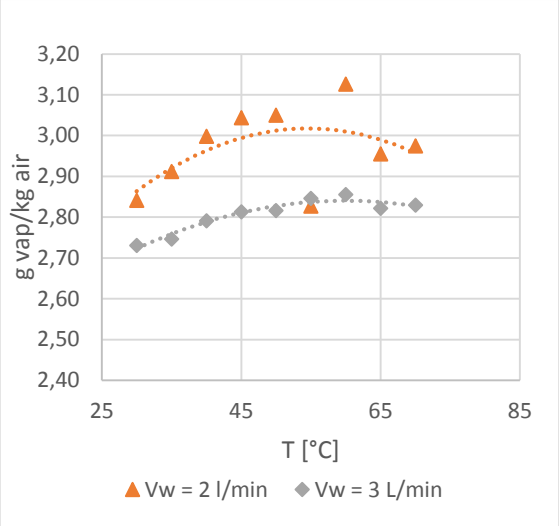


*Figure 4.15a: comparison of different water flow at constant air flow of 10 L/min, parametric in inlet flow rate*

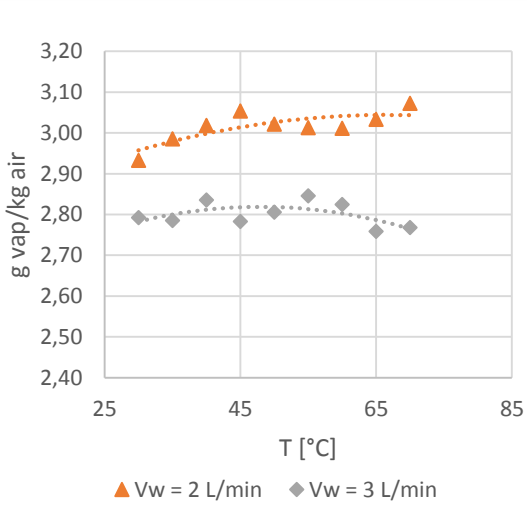


*Figure 4.15b: comparison of different water flow at constant air flow of 12 L/min, parametric in inlet water flow rate*

Moreover, Figure 4.15a and 4.15b prove again that the positive effect of air increase is not linear, but shows a maximum. This is probably linked to the residence time of fluids inside the column, i.e. to the contact time between the two phases, which is important in order to allow evaporation to take place.

### *4.2.2 Transient Period*

The second part of the analysis concerns the behaviour during transient conditions. Figures 4.16 to 4.19 show the different profiles of the amount of extracted water with time for the data obtained with a water flow rate of 2 L/min for different air flow.

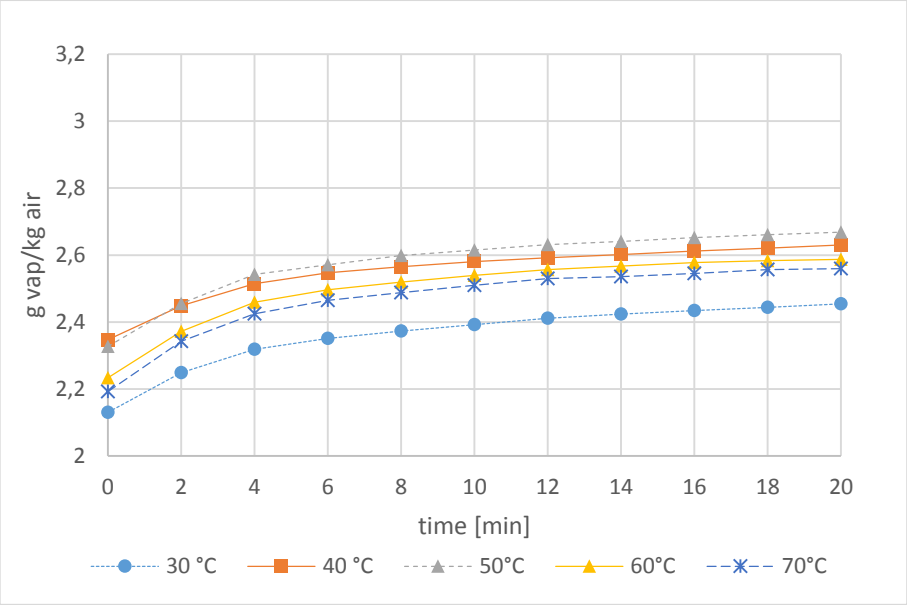


*Figure 4.16: transient behavior for 2 L/min water flow and 6 L/min air flow, parametric in inlet air temperature*

Comparing Figures 4.16 to 4.19, it is concluded that an air flow rate increase leads to a reduction of the transient time, which in any case is lower than 20 minutes. This is reasonable because the higher the air flow rate, the larger the amount of energy given to the system so that a lower time to reach the steady state is required (Riberio Jr., et al., 2004).

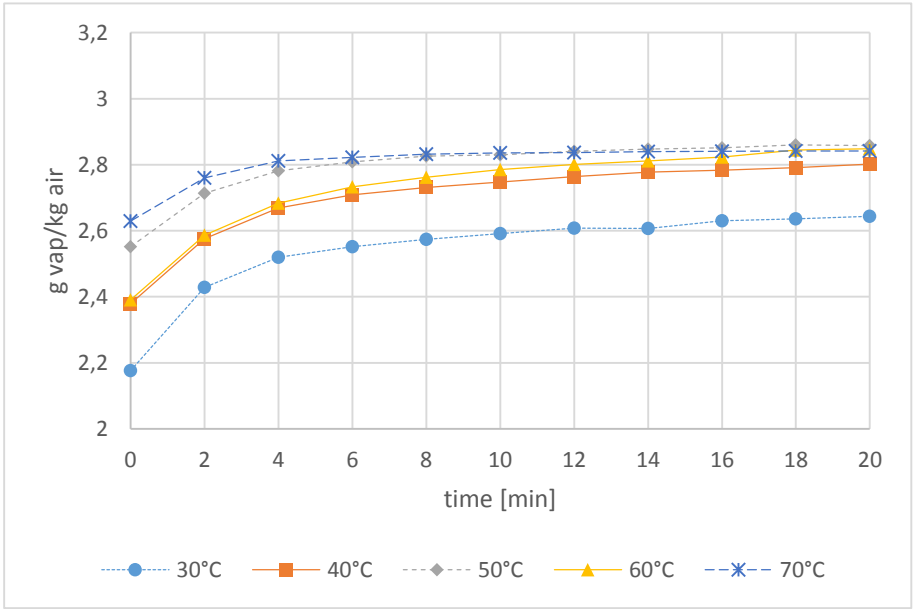


*Figure 4.17: transient behaviour for 2 L/min water flow and 8 L/min air flow, parametric in inlet air temperature*

The information resulted from steady state analysis is also embedded in dynamic one, as air flow rate and temperature effects on water extraction have been noticed since the first time of the run.

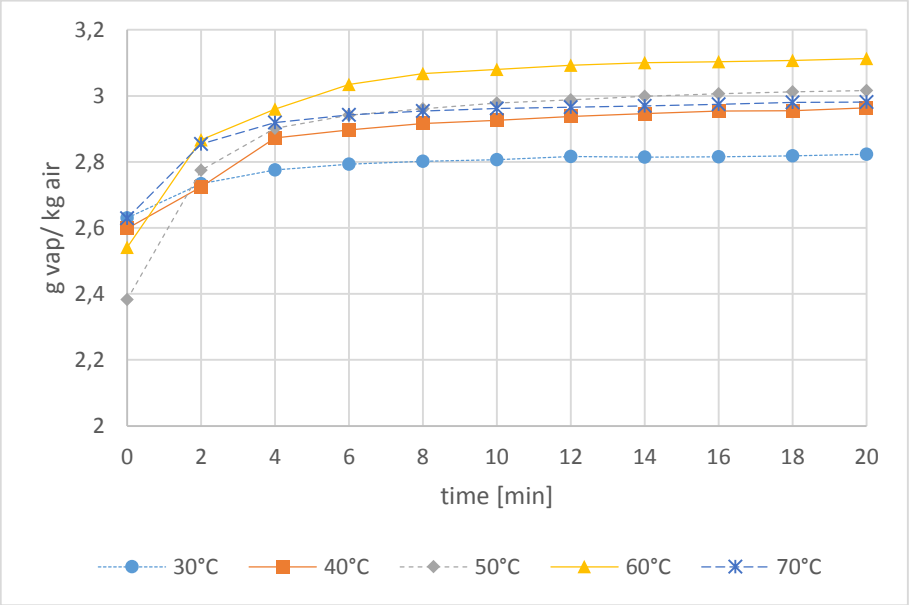


*Figure 4.18: transient behavior for 2 L/min water flow and 10 L/min air flow, parametric in inlet air temperature*

On the other hand, there are no appreciable effects of parameters on the transient time, probably because the analysed range is too small and the maximum temperature is not high enough to affect this parameter.

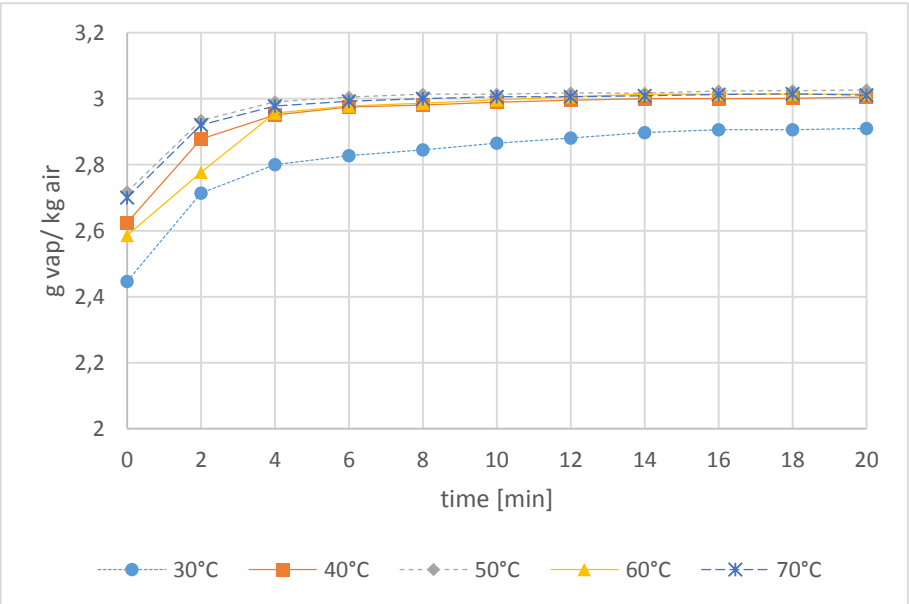


*Figure 4.19: transient behaviour for 2 L/min water flow and 12 L/min air flow, parametric in inlet air temperature*

## 4.3 Gas Holdup

It is interesting also seeing the behaviour of the gas holdup. Figure 4.20 shows the gas holdup, expressed in percent of total boiling height. As can be seen, there is no influence of water flow rate on the gas holdup, and there is a linear correlation between air flow rate and the increase of boiling level. This behaviour does not surprise, as it was already discussed and shown in Figure 2.6.

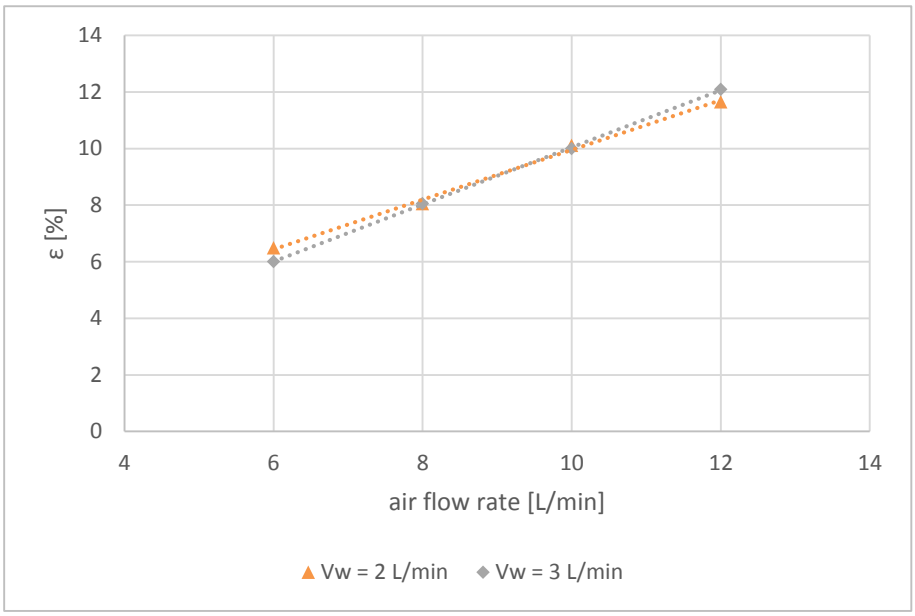


*Figure 4.20: average gas holdup, parametric in inlet water flow rate*

Also air temperature has no influence on the gas holdup, as Figure 4.21 shows. In fact, increasing the temperature the gas holdup does not increase, in contrast to expectations, because increasing temperature the gas molar volume increase and it should affect the gas holdup. Probably the temperature growth is not enough and the molar volume change is not noticeable.

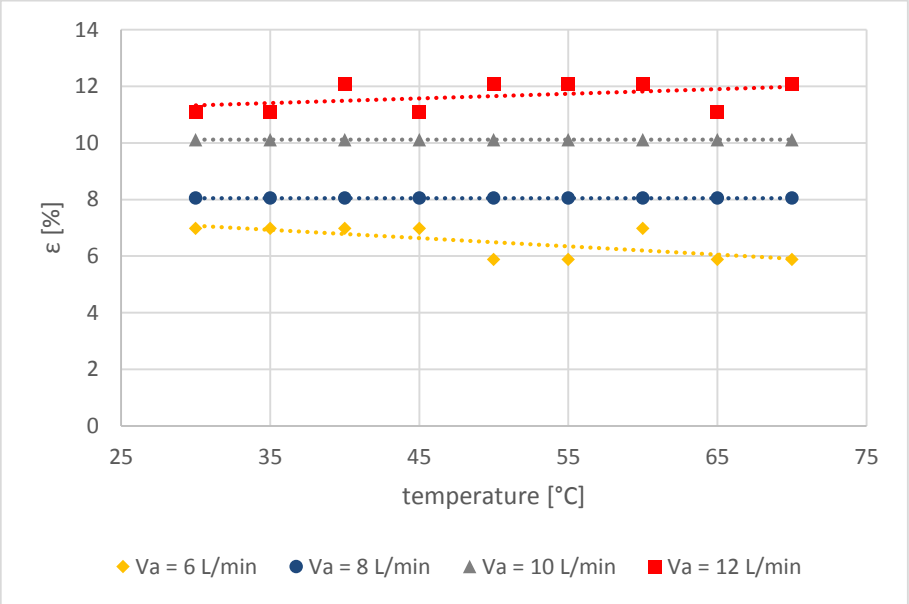


*Figure 4.21: gas holdup with temperature, for an air flow rate of 10 L/min, parametric in inlet air flow rate*

## 4.4 Hydrodynamic of the column

As reported by other authors (Riberio Jr., et al., 2005) (Boehm, 1997), the column hydrodynamic plays an important role on the heat and mass exchange, so at least a qualitative analysis on it is helpful to better understand obtained results.

It was observed during the experimental work that the system have been in the heterogeneous regime for the entire air flow rates analysed. This meant that the bubble diameter was not constant during the ascension stage, due to coalescence and breakage phenomena, but this is the best regime for heat and mass exchange, as reported in Paragraph §2.3.2. Moreover, the ascending flow is not linear, but it has a coil flow, as shown in Figure 4.22a and 4.22b.

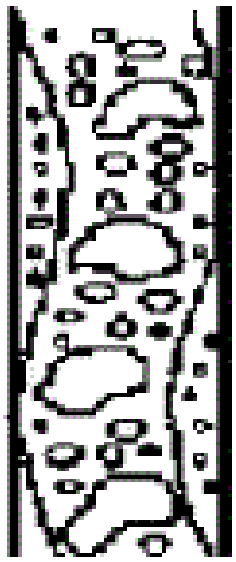

*Figure 4.22a: diagram of column hydrodynamic (Kantarci, et al., 2005)*

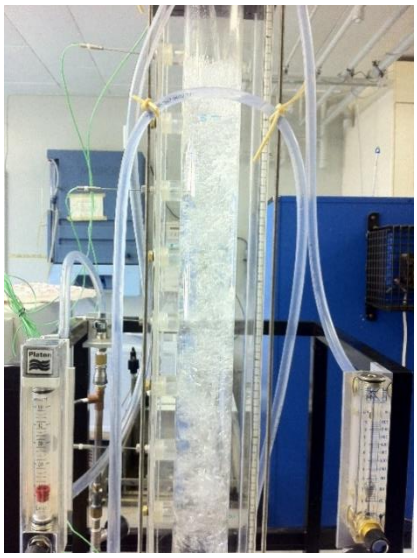

*Figure 4.22b: picture of column hydrodynamic*

Behaviour showed in Figure 4.22a is called *churn-turbulent* (Boehm, 1997) and brings to an air and water recirculation in those zones of the column outside the main coil flow.
An additional comment could be made on the bubble distribution. In fact, experiments showed that bubbles are not equally distributed on the column length, but they are more concentrate in the middle and upper part of the column, while near the sparger they are quite rare, as shown in Figure 4.23.

*Figure 4.23: picture of hydrodynamic near the sparger*

Also sparger could have had influence on bubbling regime, so to a deeper and further analysis it could be interesting analysing another kind of sparger, for example a porous sparger or one with smaller holes.

## 4.5 Final considerations

The experiments that gave the higher amount of extracted water are reported in Table 4.2.

*Table 4.2: specifications of the best experimental experiments*

| **Water flow [L/min]** | **Air flow [L/min]** | **Air temperature [°C]** | **Amount of water [g water/kg air]** |
|---|---|---|---|
| 2 | 10 | 45 | 3.04 |
| 2 | 12 | 50 | 3.05 |
| 3 | 6 | 55 | 2.9 |

Apart from these values, the most important information obtained from this work experimental work are:

- water flow rate has probably more importance than air flow rate and air temperature, at least in the range analysed;
- increasing water flow rate, extracted water decreases;
- increasing air flow rate, an opposite effect is obtained;
- increasing temperature, extracted water reaches a maximum and then decrease;
- air flow rate affects the transient time, in particular, an increase in its value is reflected in a reduction of the time;
- water and air temperatures have no influence on gas holdup, which has a linear dependence with air flow value;
- water temperature change is very low and its value is almost constant for all the experiments.

# Chapter 5

# Modelling and Comparison

In the first part of the Chapter a calculation and an analysis of the experimental heat transfer coefficient is proposed. The obtained values were compared with two published correlation and then a simple theoretical model able to predict heat transfer coefficient and temperature profile is developed.

## 5.1 Energy balance check

The simplest way to check if experimental data are accurate is to solve the energy balance using experimental data. The general formulation of the balance is:

$$\dot{Q}_W + \dot{Q}_A + \dot{Q}_{lost} = 0. \tag{5.1}$$

Where $\dot{Q}_W$ (W) is heating power exchanged by the water phase, $\dot{Q}_A$ (W) is the one exchanged by the gas phase and $\dot{Q}_{lost}$ is the heat lost due to inadequate insulation. If we assume perfect thermal insulation of the column, the balance reduces to:

$$\dot{Q}_W + \dot{Q}_A = 0. \tag{5.2}$$

Due to small water evaporation rate, it is possible to assume constant water flow rate, and a gas flow rate equal to the inlet air flow. Under this hypothesis the two terms can be expressed according to Kypritzis (Kypritzis, et al., 2001):

$$\dot{Q}_W = \dot{m}_W c_{P,W}(T_{W,out} - T_{W,in}), \tag{5.3}$$

$$\dot{Q}_A = \dot{m}_A\left[c_{P,A}\left(T_{A,out} - T_{A,in}\right) + (\omega_{out} - \omega_{in})\lambda\right]. \tag{5.4}$$

Where, $\dot{m}$ is the mass flow rate (kg/s) and $c_P$ the specific heat (J/kg °C) of water and air respectively, T is inlet and outlet column temperatures of the two phases, $\omega$ is the humidity ratio (kg of water/ kg of dry air) and $\lambda$ (J/Kg) is latent heat of water.
As mentioned in Paragraph §3.2, inlet air is dry, so $\omega_{in}$ can be set to zero, so Equation 5.4 becomes:

$$\dot{Q}_A = \dot{m}_A\left[c_{P,A}\left(T_{A,out} - T_{A,in}\right) + \omega_{out}\lambda\right]. \quad (5.5)$$

Properties of the substances needed in order to solve the balance are taken from literature and summarized in Table 5.1 (Perry, et al., 2007). After checking how their value changes with temperature, it was decided to keep them constant without making any significant error.

*Table 5.1: utilized value of air and water properties*

| $C_{P,W}$ | $P_W$ | $C_{P,A}$ | $\lambda$ |
|---|---|---|---|
| **J/kg°C** | **kg/m³** | **J/kg°C** | **J/kg** |
| 4184 | 998 | 1007 | $2257*10^3$ |

Air density was calculated from the ideal gas law at the inlet temperature:

$$\rho_A = \frac{MW*P}{R*T}\left[\frac{Kg}{m^3}\right]. \quad (5.6)$$

Where MW (kg/kmol) is the air molecular weight and P (Pa) the system pressure (1 Atm). Data accuracy were evaluated checking the percent error on the total heat exchanged:

$$E = \frac{\dot{Q}_W + \dot{Q}_A}{|\dot{Q}_W| + |\dot{Q}_A|}. \quad (5.7)$$

Figure 5.1 shows the results obtained accordingly to 5.7. It is clear that most of the errors are positive, meaning that the heat value gained by water is much higher than the one released by air and, consequently, that the system would have taken most of the energy from the surrounding. This is impossible due to the system insulation, so a better explanation is that water temperature change is so low (half a degree), that thermocouples sensibility is inadequate to measure accurately this change.

To obtain an accurate value it is suggested to repeat this experiments with more accurate instrumentation or with a bigger column, in which greater water temperature changes can be achieved. However, the goal of this work was to determine a profile of water extraction rather than a water temperature profile.

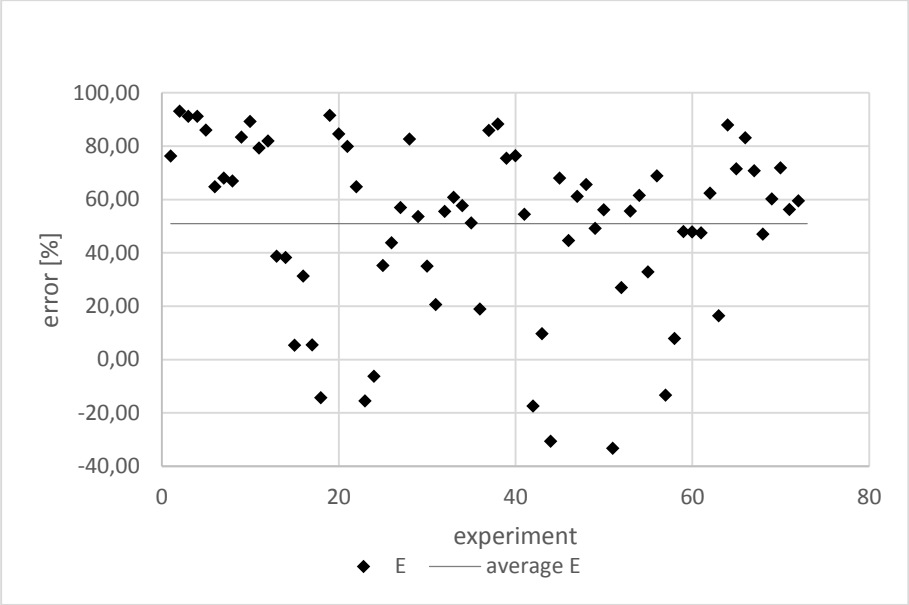


*Figure 5. 1: error percentage distribution*

## 5.2 Experimental Heat Transfer coefficient

Starting from the experimental data, the experimental overall heat transfer coefficient was calculated for all the experiments. Calculation started from the definition of the heat transfer coefficient:

$$U = \frac{\dot{Q}}{\Delta T_{ml} A} , \tag{5.8}$$

Where U is the overall heat transfer coefficient (W/ $m^2$ °C), $\dot{Q}$ (W) is the heat power exchanged, $\Delta T_{ml}$ is the logarithmic mean temperature difference (°C) and A the exchange area ($m^2$).

For the calculation of the temperature difference it the value of the water outlet temperature is needed. Due to errors discussed in the previous section, it was decided to obtain this value from the water energy balance (Equation 5.3) using as a correct power value the one measured on gas side (Equation 5.5).

Exchanged heat can be expressed by using Equation 5.5, and substituting $\dot{Q}$into 5.8, it is obtained:

$$U = \frac{\dot{m}_A [c_{P,A}(T_{A,out} - T_{A,in}) + \omega_{out}\lambda].}{\Delta T_{ml} A}, \tag{5.9}$$

The last needed parameter is the exchange area, which was calculated in two different ways, one based on the total area, the other one starting from the single drop dimension. The two calculations are presented below.

### *5.2.1 Total surface area*

The interfacial area A is calculated starting from column diameter and gas hold up:

$$A = A_C * \varepsilon, \tag{5.10}$$

where $A_c$ ($m^2$) is the column cross section area and ε is the gas holdup, defined in Equation 2.9. Figure 5.2 and 5.3 show the experimental heat transfer coefficient obtained using Equation 5.1. ε data point are reported in Figure 4.20 and 4.21.

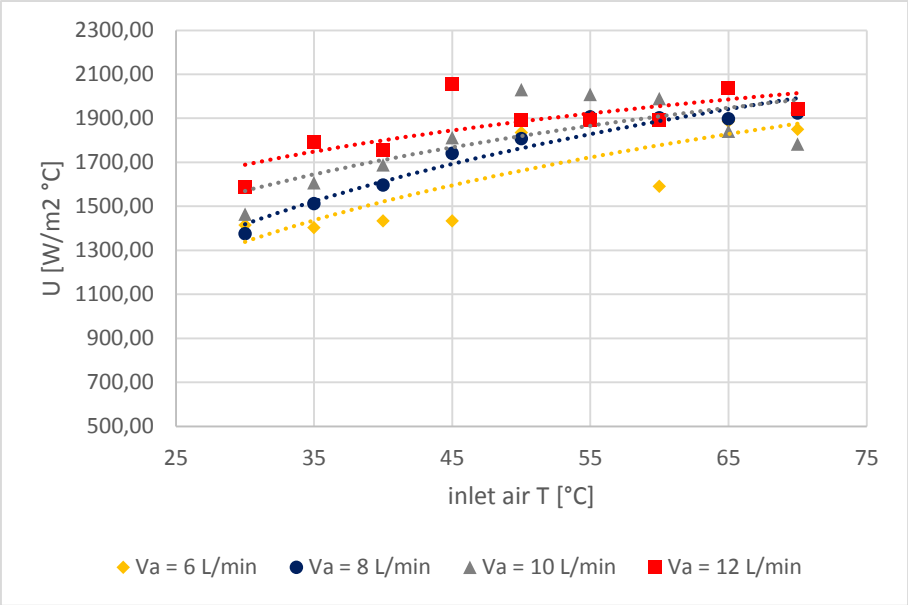


*Figure 5.2: experimental heat transfer coefficient for a water flow rate of 2 L/min, parametric in inlet air flow rate*

By comparing the two figures it can be seen that in both cases there are no substantial differences between the two water flow rates, and that the coefficient increases with increasing inlet air temperature. It is also clear that the air inlet flow rate has no particular effect on the heat transfer coefficient as well.

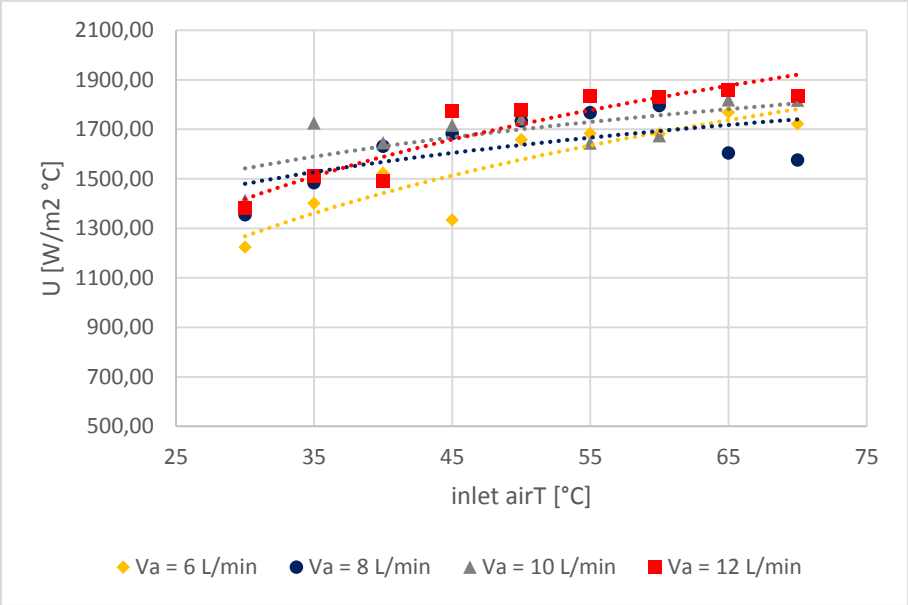


*Figure 5.3: experimental heat transfer coefficient for a water flow rate of 3 L/min, parametric in inlet air flow rate*

## 5.2.2 Area of a drop

In order to obtain the interfacial area of a single drop, it is necessary to calculate bubble diameter. Although many correlations developed for this purpose, it was used the one reported by Kantarci (Kantarci, et al., 2005), which holds for low gas flow rates:

$$d_b = \left[\frac{6\pi d_0}{g(\rho_W - \rho_A)}\right]^{1/3}, \tag{5.11}$$

where $d_b$ (m) is the bubble diameter, $d_0$ is the orifice diameter and $g$ (9.81 m/s$^2$) is the acceleration of gravity. For this calculation air and water density have been kept constant along the column, so also the bubble diameter is constant along the column. Moreover, all bubbles are considered as spherical and with the same size, and phenomena of coalescence and breakage are not taken into account.

The area of a bubble ($A_b$) is then calculated from:

$$A_b = \pi {d_b}^2. \tag{5.12}$$

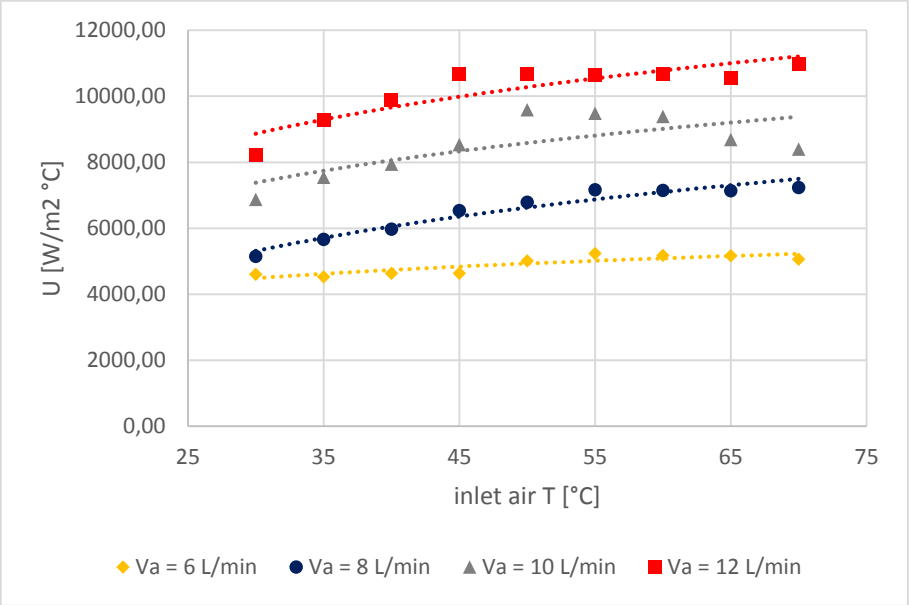


*Figure 5.4: experimental heat transfrer coefficient for a water flow of 2 L/min, parametric in inlet air flow rate*

Figure 5.4 and 5.5 show the experimental heat transfer coefficient obtained using the bubble surface as interfacial area. It can be seen that water flow rate has no substantial influence on its value, while the other parameters show a similar influence on coefficient value. In particular, an increase of air flow rate, at constant other conditions, causes an increase of the calculated coefficient, while a temperature increase brings to an increase of the coefficient as well, even though this influence seems to be less important than air's velocity one. Moreover, at higher temperatures the heat exchange coefficient value seems to reach a stable value. Comparing this result with Table 4.2 and results shown in Chapter 4, it can be noticed that the best results were obtained when the coefficient is approaching its maximum value, between temperatures of 45-55 °C.

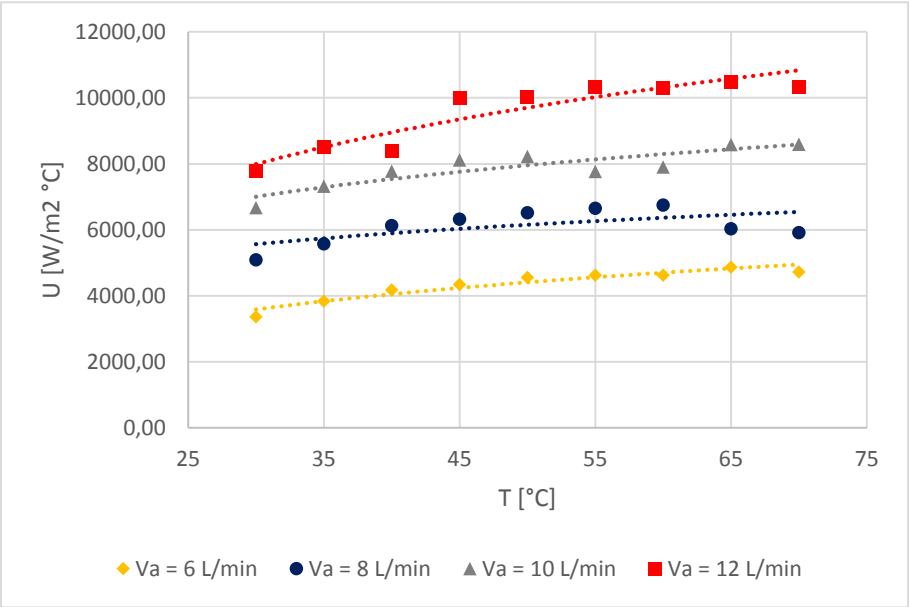


*Figure 5.5: experimental heat transfrer coefficient for a water flow of 3 L/min, parametric in inlet air flow rate*

This two results are reasonable, because a higher air flow rate means more turbulence inside the column causing a greater liquid recirculation, and so higher contact time and so a better exchange. Increasing the temperature means increase the driving force, and so the total amount of exchangeable heat.

## 5.3 Heat transfer coefficient modelling

The experimental heat transfer coefficient were then compared with two existing correlations published in the literature. The first one was proposed by Mahood (Mahood, et al., 2013), the second one by Kang (Kang, et al., 2002).

Mahood's a correlation calculates the Nusselt number (Nu) based on gas holdup and Peclet number (Pe):

$$Nu = \frac{4}{\sqrt{6\pi}}\left(\frac{\varepsilon+0.5}{1-\varepsilon}\right)^{0.5} Pe^{0.5}. \tag{5.13}$$

In this correlation Nu and Pe are defined:

$$Nu = \frac{2d_b U}{k_w}, \tag{5.14}$$

$$\mathrm{Pe} = \frac{2d_b v_r}{\alpha_w}; \tag{5.15}$$

where $k_w$ (W/mK) is the thermal conductivity of water, $\alpha_w$ ($m^2/s$) is the thermal diffusivity of water, and $v_r$ is the relative velocity between the two phases, and expressed by:

$$v_r = \frac{v_0}{2}\left[\frac{(1-\varepsilon)^3}{\varepsilon+0.5}\right], \tag{5.16}$$

where $v_0$ is the relative velocity of a single drop, as defined by:

$$v_0 = \frac{2g\rho_w d_b^2}{9\mu_w f_{Re}}, \tag{5.17}$$

$$f_{Re} = 1 + 0.15\mathrm{Re}^{0.687}, \tag{5.18}$$

$$\mathrm{Re} = \frac{\rho_w d_b v_r}{\mu_w}. \tag{5.20}$$

In Equation 5.17, μ (Pa s) is the water viscosity and the bubble diameter is calculated from Equation 5.11.
Kang's correlation predicts the heat transfer coefficient for a single drop accordingly:

$$Nu_b = 3.1Re_b^{0.37}Pr_w^{1/3}, \tag{5.21}$$

where $Re_b$ is the Reynolds number of the droplet, $Pr_w$ is water Prandtl number and $Nu_b$ is bubble Nusselt number, defined as:

$$\mathrm{Re}_b = \frac{\rho_a d_b v_r'}{\mu_a}, \tag{5.22}$$

$$\mathrm{Nu}_b = \frac{d_b U_b}{k_a}, \tag{5.23}$$

$$Pr_w = \frac{c_{P,w}\mu_w}{k_w}. \tag{5.24}$$

$k_a$ is air thermal conductivity and $v_r'$ is the relative velocity between the phases.
This relative velocity is defined as the difference between water and bubble velocity, which are obtained as follow:

$$v_b' = \frac{\dot{V_A}}{\varepsilon * A_C}; \tag{5.25}$$

$$v_w = \frac{\dot{V_w}}{(1-\varepsilon) * A_C} \tag{5.26}$$

where $V_A$ and $\dot{V_w}$ ($m^3/s$) is the volumetric flow rates of air and water respectively.

## 5.4 Coefficients comparison

The results obtained with the two models were compared with the experimental values of heat transfer coefficients. In the case of Mahood's model the comparison was made with the total heat transfer coefficient, for Kang's one with the coefficient of a single drop.

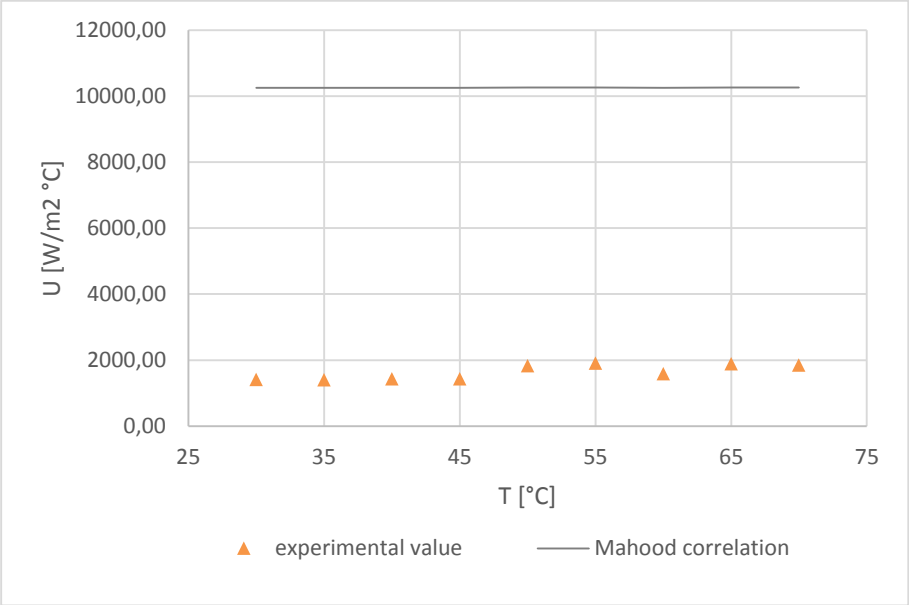


*Figure 5.6: comparison between experimental coefficient and Mahood correlation for the heat transfer coefficient*

Figure 5.6 shows the comparison of Mahood's results: clearly the model does not reproduce the experimental values. This mismatch could be due to a wrong estimation of relative velocity, which brings to a high *Pe* value, and consequently, to a great *Nu* number. Figure 5.7 shows the comparison with Kang's correlation, showing better results, especially for low air flow rates (6-8 L/min). In this range the difference between calculated and experimental results is almost 25%.
At higher air flow rates also this model is not able to fit very well experimental results.

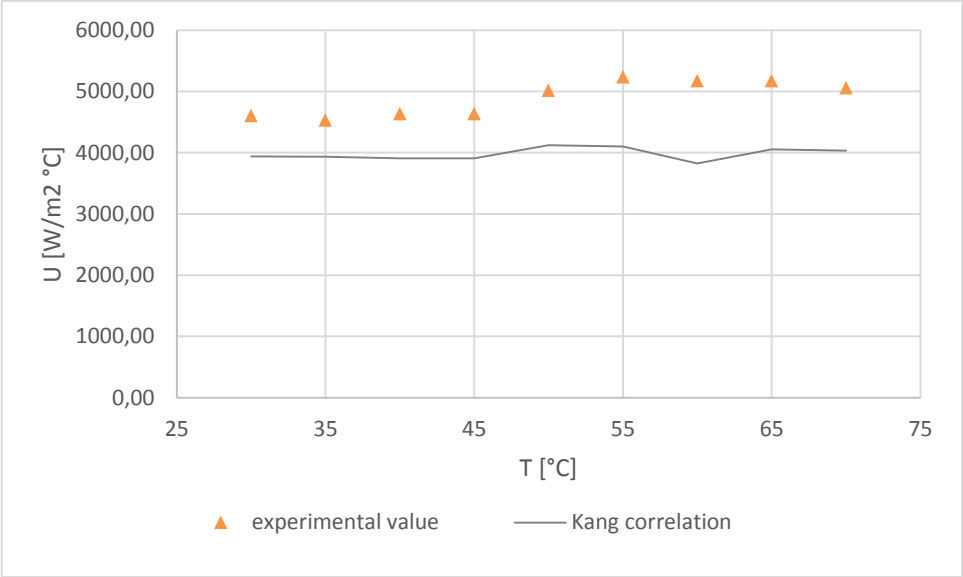


*Figure 5.7: comparison between experimental coefficient and Hang correlation for the heat transfer coefficient*

This increasing error for high air flow rates could be due to the assumption made on bubbles: spherical shape, constant diameter and no breakage. Kang's correlation showed a great sensitivity to bubble diameter, so probably a more accurate estimation of this parameter could improve the results.

## 5.5 Model application

In order to verify if the existing coefficient correlations is useful to predict the air temperature inside the column, it was applied Kang's correlation to the experimental runs that has a better match. In this work it is reported only a sample of this application, whose initial conditions are reported in Table 5.1.

*Table 5.1: characteristics of the simulated experiment*

| **Water flow rate [L/min]** | **Air flow rate [L/min]** | **Air inlet temperature [°C]** |
|---|---|---|
| 3 | 6 | 55 |

Following Kang's suggestion (Kang, et al., 2002) the differential energy balance was written for the air temperature, considering as constant both the mass flow rate and the specific heat capacity. Moreover, looking at experimental results, it was decided to take

water temperature as a constant, so that the energy balance on water side reduces to an identity, and its formulation was not necessary. The resulting equation is:

$$\dot{V}_A \rho_A c_{p,A} T_A\big|_z - \dot{V}_A c_{p,A} \rho_A T_A\big|_{z+\Delta z} - A_g U_b (T_A - T_W) = 0, \tag{5.27}$$

where $U_b$ is the calculated coefficient by the Kang's correlation, $A_g$ is the total area of bubbles, defined as:

$$A_g = N_b A_b, \tag{5.28}$$

where $N_b$ is the total number of bubbles, defined as:

$$N_b = \frac{6 A_C \varepsilon \Delta z}{\pi {d_b}^3}. \tag{5.29}$$

Substituting Equation 5.29 into 5.28, it was obtained:

$$A_g = \frac{6 \varepsilon A_C}{db} \Delta z, \tag{5.30}$$

In 5.27 $\dot{V}_A \rho_A$ can be expressed as

$$\dot{V}_A \rho_A = \dot{m}_A, \tag{5.31}$$

Substituting 5.31 and 5.30 into 5.27, dividing it by $\Delta z$, and differentiating the result, the final equation is obtained:

$$\frac{\mathrm{d}T_A}{\mathrm{dz}} = -\frac{A_b U_V (T_A - T_W)}{\dot{m}_A c_{P,A}}. \tag{5.32}$$

$U_V$ [W/m3°C] is the volumetric heat transfer coefficient, defined as:

$$U_V = 6 \frac{\varepsilon}{d_b} U_b, \tag{5.33}$$

After integrating and rearranging Equation 5.31, the final Equation was obtained:

$$T_A = T_W + \left(T_A^{in} - T_W\right) e^{-Cz}, \tag{5.34}$$

$$C = \frac{A_c U_V}{\dot{m}_A c_{P,A}}, \tag{5.35}$$

where z (m) is the column axial coordinate.

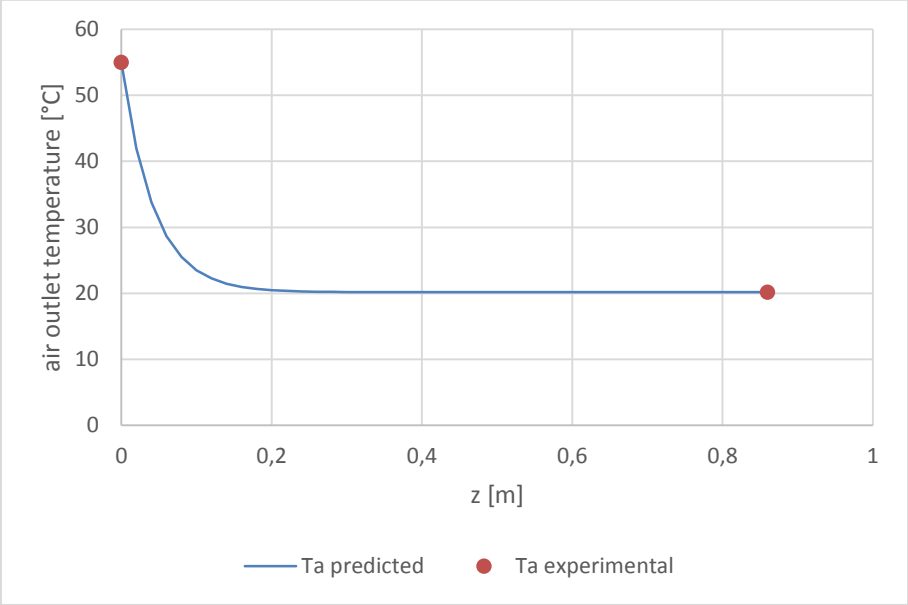


*Figure 5.8: application of Kang model to an experimental run*

Figure 5.8 shows that in this case the predicted profile (continue line) matches the experimental values (dots). It is recalled that between air outlet temperature and water inlet one there is not a substantial difference, and so it is possible that this had influenced the prediction.

Referring to simulation carried out by Kang (Kang, et al., 2002), it was then decided to apply the developed model to simulate a column with larger diameter ($D_C$ = 1 m) and bubbling height of 85 cm, maintaining the same water and air velocities, which means maintain constant both the gas holdup and Nusselt number. The inlet air temperature was fixed to T = 55°C, while water one was set on T=20°C. Air and water flow rate were calculated using Equations 5.18, obtaining $\dot{V}_A = 0.020$ m$^3$/s and $\dot{V}_W = 0.010$ m$^3$/s.

The sparger of the column was also designed considering that the velocity at the orifice:

$$v_o = \frac{\dot{V}_A}{A_o}, \tag{5.36}$$

is kept equal to the experimental case.

Then the total orifice area necessary for the new sparger was calculated simply substituting the new water volumetric flow rate and rearranging the 5.23.

It was obtained $A_o$ = 0.02 m$^2$. Under the assumption that the available spargers have same orifice diameter and same number of orifices, it was calculated that 204 spergers are needed. If the spargers have the same diameter of the ones used in the experimental work

(6 cm), they can be placed in the column with a pitch to diameter ratio p/d = 0.27 (Sinnot, et al., 2009).
The resulting air profile temperature in the column is shown in Figure 5.9.

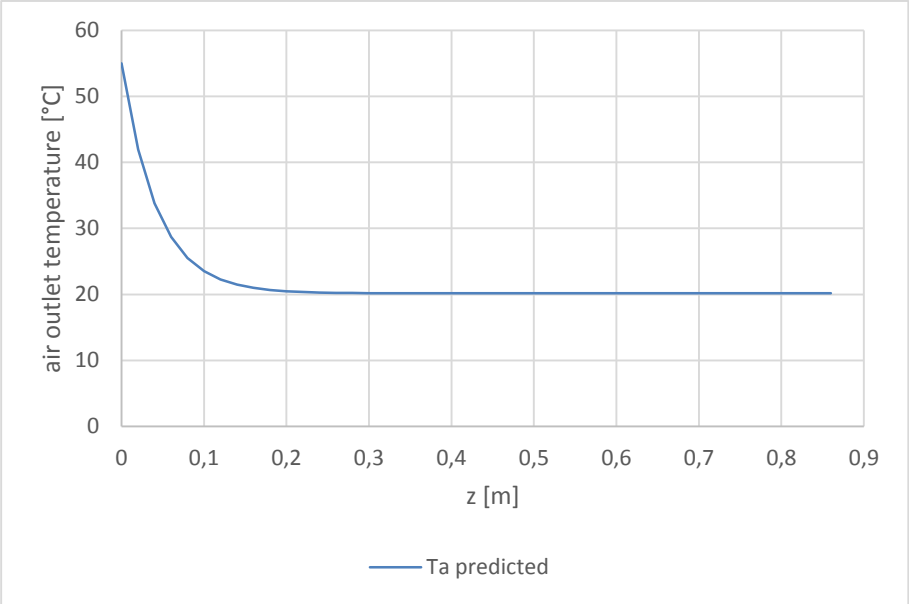


*Figure 5.9: application of the model with Kang correlation for a temperature prediction*

To calculate the amount of water extracted, it was assumed saturation in the outlet air stream, as shown by experiments. Based on the calculation reported in Paragraph §2.2.1, 3 g of water are extracted for kg of air, which brings to 241 g/h of water evaporation.

The predicted air temperature profile is equal to the one obtained from the experimental run simulation. This behaviour is does not surprise because of the way in which air flow rate is obtained. In fact is defined as 5.25, and in this term the only variable is $A_c$, substituting 5.25 into 5.35 it is obtained:

$$C = \frac{U_V}{\rho_A c_{P,A} v_b' \varepsilon}, \tag{5.37}$$

which is made of terms that are kept constant between the two simulations.
Moreover, as can be seen from Figure 5.9, most of the column height is unused, as the final temperature is reached approximately after one third of the high.
A better solution would be use of pans with larger diameter and low bubbling height rather than high columns.

# Conclusions

The aim of this work was to investigate the influence of process parameters in a humidification column for water desalination, and find a simple model able to predict air temperature profile.

The effects of air and water flow rate and air inlet temperature to the internal water temperature profile and amount of water extracted with the exit gas stream were investigated. This study was divided into two parts, an experimental and a theoretical one. Experiments were carried out to analyse all the combinations of the parameters values: for water flow rates of 2 and 3 L/min were considered, whereas air effects were analysed from 6 to 12 L/min with a step of 2 L/min, and air inlet temperature was from 30 to 70 °C with a step of 5 °C. The theoretical part of the work includes a calculation of the experimental heat transfer coefficient and a comparison with values obtained with existing correlations. In the last part of the work a simple model was developed, which is able to predict the air outlet temperature.

The obtained experimental results showed that all the parameters analysed influences the amount of extracted water, but the internal profile temperature was almost constant for all the runs, and water temperature change along the column was less than half of degree for all the runs.

As about the influence on exit air humidity, it was noticed that there are interactions among all parameters. With all other conditions constant, increasing air inlet temperature brings to an increase of water in the air exit flow. For low air flow rate (6 and 8 L/min) an increase of air flow rate has positive effect on the water extraction, while for higher values (10 and 12 L/min) this effects disappear.

Also water flow rate has effects on the humidity of air outlet stream, in particular an increase of water flow rate decreases the amount of extracted water.

Experimental data were then checked and verified with the energy balance, obtaining a high percent errors, which are due to instrument insufficient accuracy. In fact, the water temperature changes were small and thermocouples were not able to detect it well. It was observed that a small error in the measurement could bring to an overestimation of the exchanged heat in the water side.

The calculated experimental heat transfer coefficient were compared with those calculated with two different correlation, obtaining a good match, at least for low gas flow rate, with the correlation proposed by Kang (Kang, et al., 2002), while the one proposed by Mahood is inefficient.

A model was developed and an experimental case were simulated, obtaining a good match with the final temperatures. Then this model was used to predict the air temperature profile with a column with industrial diameter. This brings to the conclusion that pans with larger diameter and low water height should be used instead of high columns.

The main limit in the experimental analysis is that water temperatures were almost constant, regardless the values used for the process parameters.

Other difficulties were found in the water flow rate control of the feed pump, whereby it was not possible to analyse a larger range. Another relevant limit is that only tap water was tested, and salt effect on the heat transfer coefficient were not investigated.

As about the simulation model, the hypothesis made on the spherical shape of the bubbles, with no breakage nor coalescence phenomena, constant dimension and rising velocity are too rough.

Further work should address, first of all, the equipment performances with a salt water feed and, with higher inlet air temperatures, closer to a real industrial case. Another possible improvement is using a packing inside the column, which generally increases the heat transfer coefficient.

# Nomenclature

$\dot{Q}$ = exchanged heat rate (W)
$\dot{m}$ = mass flow rate (kg/s)
A = surface ($m^2$)
C = molar concentration ($kmol/m^3$)
$C_P$ = heat capacity (J/kg K)
$D_A$ = water diffusivity ($m^2/s$)
$d_b$ = bubble diameter (m)
$D_c$ = column dimater (m)
E = error (%)
H = high of liquid (m)
l = membrane thickness (m)
M = mass (kg)
$N_A$ = molar flux (kmol/s)
P = pressure (Pa)
$Q_F$ = feed flow rate ($m^3/s$)
$Q_P$ = permeate flow rate ($m^3/s$)
R = ideal gas law constant (J/kmol K)
$R_w$ = freshwater recovery
S = water solubility (kmol/kmol)
T = temperature (K)
U = overall heat transfer coefficient ($W/m^2K$)
$U_V$ = volumetric overall heat transfer coefficient ($W/m^3K$)
v = velocity (m/s)
V = water partial molar volume ($kmol/m^3$)
Nu = Nusselt number
Pe = Peclet number
Re = Reynolds number
Pr = Prandtl number

Greeks letter

α = thermal diffusivity ($m^2/s$)
μ = viscosity (Pa s)
Δ = difference
ε = gas holdup

$\lambda$ = water heat of vaporization (J/kg)
$\Pi$ = osmotic pressure (Pa)
$\rho$ = density (kg/m$^3$)
$\omega$ = humidity ratio

## Acronyms

ED = electrodialysis
HD = humidification dehumidification
MED = multiple effect distillation
MOD = manipulated osmosis desalination
MSF = multi-stage flash distillation
MW = molecular weight
NF = nanofiltration
RH = relative humidity
RO = reverse osmosis
TDS = total dissolved salt
VCD = vapour compression distillation

## Subscripts

0 = single bubble
a = air
b = bubble
r = relative
w = water

# References


Bourouni, K., M. T. Chaibi, e L. Tadrist. «Water desalination by humidification and dehumidification of air: state of art.» *Desalination 137*, 2001: 167-176.

Mahmoudi, Hacene, Nawel Spahis, e Mattheus F. Goosenc. «Application of geothermal energy for heating and fresh water production in a brackish water greenhouse desalination unit: A case study from Algeria.» *Renewable and Sustainable Energy Reviews 14*, 2010: 512-517.

Paul, D. R. «Reformulation of the solution-diffusion theory of reverse osmosis.» *Journal of membrane science 241*, 2004: 371-386.

Sadrzadeh, Mohtada, e Toraj Mohammadi. «Sea water desalination using electrodialysis.» *Desalination 221*, 2008: 440–447.

Alnaimat, F., J. F. Klausner, e R. Mei. «Transient analysis of direct contact evaporation and condensation within packed beds.» *International Journal of Heat and Mass Transfer 54*, 2011: 3381-3393.

Al-Sahali, Mohammed, e Hisham Ettouney. «Development in thermal desalination processes: Design, energy, and costing aspects.» *Desalination 214*, 2007: 227-240.

Bird, R. B., W. E. Steward, e E. N. Lightfoot. *Transport phenomena.* New York: John Wiley & Sons, Inc, 2007.

Boehm, Robert F. «Direct contact heat transfer.» Chapter 19. Las Vegas: University of Nevada, 1997.

Boulana, K., N. Galanis, e J. Orfi. «Heat and mass transfer between gas and liquid streams in direct contact.» *International Journal of Heat and Mass Transfer 47*, 2004: 3669-3681.

Diawara, Courfia K. «Nanofiltration process efficiency in water desalination.» *Separation & purification reviews 37:3*, 2008: 302-324.

El-Agouz, S. A. «Desalination based on humidification-dehumidification by air bubbles passing through brackish water.» *Chemical Engineering Journal 165*, 2010: 413-419.

El-Agouz, S. A., e M. Abugderah. «Experimental analysis of humidification process by air passing through seawater.» *Energy Conversion and Management 49*, 2008: 3698-3703.

El-Ghonemy, A. M.K. «Future sustainable water desalination technologies for the Saudi Arabia: a review.» *Renewable and Sustainable Energy Reviews 16*, 2012: 6566-6597.

Eslamimanesh, A., e M. S. Hatamipour. «Mathematical modeling of a direct contact humidification-dehumidification desalination process.» *Desalination 237*, 2009: 296-304.

Eslamimanesh, A., e M. S. Hatamipour. «Mathematical modeling of a direct contact humidification-dehumidification desalination process.» *Desalination 237*, 2009: 296-304.

Eslamimanesh, A., e M. S. Hatamipour. «Mathematical modeling of a direct contact humidification-dehumidification desalination process.» *Desalination 237*, 2009: 296-304.

Fritzmann, C. , J. Löwenberg, T. Wintgens, e T. Melin. «State-of-the-art of reverse osmosis desalination.» *Desalination 216*, 2007: 1-76.

Gatto, Damiano. *Experimental investigation of ethanol separation by reverse osmosis.* Universita' degli studi di Padova: Tesi di laurea magistrale in Ingegneria chimica e dei Processi Industriali. DIPIC, 2012.

Greenlee, Lauren F., Desmond F. Lawler, Benny D. Freeman, Benoit Marrot, e Philippe Moulin. «Reverse osmosis desalination: Water sources, technology, and today's challenges.» *Water research 43*, 2009: 2317-2348.

Hashemifard, S. A. , e R. Azin. «New experimental aspects of carrier gas process (CGP).» *Desalination 164*, 2004: 125-133.

Hermosilo, Juan-Jorge , e Camilo A. Arancibia-Bulnes. «Water desalination by air hmidification: Mathematical model and experimental study.» *Solar Energy 86*, 2012: 1070-1076.

Kang, Yong Heack, Nam Jin Kim, Byung Ki Hur, e Chong Bo Kim. «A numerica study on heat transfer caracteristics in a spray column direct contact heat exchanger.» *KSME International Journal* 16, n. 3 (2002): 344-353.

Kantarci, N., F. Borak, e K. O. Ulgen. «Bubble Column Reactors review.» *Process Biochemistry 40*, 2005: 2263-2283.

Kypritzis, Sofoklis, e Anastasios J. Karabelas. «Direct contact air-water heat transfer in a column with structured packing.» In *Experimental Heat Transfer, fluid mechanics, and thermodinamics*, a cura di 2001 Edizioni ETS, 1695-1700. Pisa, 2001.

Li, Xingang, Shaoqing Liu, Xiaoti Cui, e Hong Li. «Experimental study of direct contact steam condensation in structured packing.» *Asian-Pacific Journal of Chemical Engineering*, 2013.

Mahood, Hameed B., Adel O. Sharif, Ali Seyed Hosseini, e Rex B. Thorpe. «Analytical modelling of a Spray column trhee-phase direct contact heat exchanger.» *ISNR Chemical Engineering* 2013 (2013).

Perry, Robert H., e Don W. Green. *Perry's chemical Engineers' Handbook, 8th edition.* 2007.

Riberio Jr., Claudio P., e Paulo L. C. Lage. «Direct-contact evaporation in the homogeneous and heterogeneous bubbling regimes. Part I: experimental analysis.» *International Journal of Heat and Mass Transfer 47*, 2004: 3825-3840.

Riberio Jr., Claudio P., e Paulo L. C. Lage. «Gas-Liquid Direct-Contact Evaporation: A Review.» *Chemical Engineering Technology 28*, 2005: 1081-1107.

Saidur, R., E. T. Elcevvadi, S. Mekhilef, A. Safari, e H. A. Mohammed. «An overview of different distillation methods for small scale applications.» *Renewable and Sustainable Energy Reviews 15*, 2011: 4756– 4764.

Wijimans, J. G., e R. W. Baker. . «The solution-diffusion model: a review.» *Journal of membrane science 107*, 2005: 1-21.

Web sites:

http://blogs.cfr.org/patrick/2012/05/08/not-a-drop-to-drink-the-global-water-crisis/?cid=oth_partner_site-atlantic (last seen 29/03/2013)

http://www.interactioncouncil.org/world-confronts-serious-water-crisis-former-heads-government-and-experts-warn-new-report (last seen 29/03/2013)

http://www.bbc.co.uk/news/magazine-17600062 (last seen 2/4/2013)

# Acknowledgements

Siamo giunti alla fine di questo lungo percorso, ricco di difficoltà ma anche tante soddisfazioni.

*Prima di iniziare la carrellata di ringraziamenti, vorrei dedicare questo mio approfondito e lungo lavoro a mio fratello Marco, per essere una presenza silenziosa ma costante e, nonostante la sua giovine età, sempre capace di dare buoni consigli.*

Non sarei arrivato dove sono ora se non fosse stato per la mia famiglia, che desidero ringraziare vivamente; non serve che vi dica molte parole, non sarebbe da me e sarebbero superflue e scontate, mi limito a un: GRAZIE Papà e Mamma.
Ringrazio inoltre il Prof Alberto Bertucco, che ha seguito il mio lavoro e corretto il mio non sempre perfetto inglese (so che per lei è un dovere e un piacere, ma io la ringrazio lo stesso).
Un grazie speciale anche a tutte le persone che mi sono state accanto durante il mio percorso, a quelle che si sono perse per strada e a quelle che, seppur in poco tempo, sono diventate molto importanti. Dicendo questo non posso non pensare a Elena, compagna di avventure/sventure in quel di Guildford (sempre uniti contro il pirla). Grazie a Luca, per le foto dell'Erasmus e le grandi camminate ( ☺ ). Quella con voi è un'amicizia nata un po' per caso, per "dovere" se vogliamo dirla, ma si è poi trasformata in un'amicizia vera e sincera, che sono sicuro durerà mooooolto a lungo.
Pensando ad amicizie nate per caso, non si può non menzionare Domenico, Silvio, Giacomo, Tommaso e il già citato Luca, membri del Surrey Summer Village, per aver sempre reso le mie serate memorabili, di ogni evento si potrebbe scrivere un libro: grazie ragazzi. Lo spirito del nostro piccolo/grande gruppo sono sicuro resterà per sempre.
Non posso non dire grazie al *Jumping che cazzo group* al *Group sex and more* (divenuto poi *Virtual fuck with us*), in particolare grazie a Marta, Martina, Tamy e, ultima ma non ultima, Anaïs (per ovvi motivi).
Accanto ai nuovi amici, ci sono quelli che mi hanno accompagnato sin dall'inizio di questa avventura o si sono aggiunti nel percorso, grazie a me *compare* Cristian, sempre presente anche se la vita ci ha portato ad avere strade diverse; a Matteo, Enrico, Tony, Michele, Luca R, ed i famosi Luca M., Luca K., che purtroppo non possono essere presenti.
Con questa frase posso davvero dire che si chiude un capitolo molto importante della mia vita, ma ne inizierà un altro ancora più ricco di soddisfazioni (e qualche responsabilità)..